

IMPACT OF PRECIPITATION CHARACTERISTICS IN NUTRIENT  
AND CARBON DELIVERY TO STREAMS IN ARTIFICIALLY  
DRAINED LANDSCAPES OF THE MIDWEST

Pilar E. Cuadra

Submitted to the faculty of the Indiana University  
in partial fulfillment of the requirements  
for the degree  
Master of Science  
in the Department of Earth Sciences,  
Indiana University  
December 2009

Accepted by the Faculty of Indiana University, in partial fulfillment of the requirements for the degree of Master of Science.

---

Philippe G. Vidon, Ph.D., Chair

---

Pierre-Andre Jacinthe, Ph.D.

Master's Thesis  
Committee

---

Todd V. Royer, Ph.D.

## ACKNOWLEDGEMENTS

I would like to thank my family, especially my parents, who were always there for me despite being more than 2000 miles away -This accomplishment is more yours than mine. I would also like to thank Ryan – there are no words to express how thankful I am for all your love and support throughout the last two years.

Thanks also to my advisor Philippe, for your patience and your support from beginning to end, for believing in me and for giving me this great opportunity. Thanks also to the remainder of my committee, Dr. Pierre-Andre Jacinthe and Dr. Todd V. Royer, for your great contributions and suggestions through the duration of this project. To Matt Hennessy for all the help and support in every stage of this research. To Lani Pascual for all the help and support in the lab. To Peter Sauer for helping with the sample analysis.

I am sincerely grateful to Dr. Arthur and Patricia Mirsky for the fellowship they provided me for the past year, and to the USGS and the Indiana Water Resources Research Center for the research grants they awarded Dr. Philippe Vidon. Without your support this project would not have been possible.

## ABSTRACT

Pilar Cuadra

### IMPACT OF PRECIPITATION CHARACTERISTICS IN NUTRIENT AND CARBON DELIVERY TO STREAMS IN ARTIFICIALLY DRAINED LANDSCAPES OF THE MIDWEST

Although many studies have investigated the impact of tile drainage on nitrate and pesticide export from cropland to streams, little information is known about the primary hydrological controls of tile flow response to precipitation events and its impact on N, P and C transport in artificially drained landscapes of the US Midwest. This study investigated 1) the relationship between precipitation characteristics and tile flow response at a high temporal resolution during storms; 2) the relative importance of macropore and matrix flow in tile flow and in N, P and C transport to tile drains; and 3) the impact of storm characteristics in N, P and C fluxes/export rates. The study was conducted between April and June 2008, in an agricultural tile drained soybean field, representative of agro-ecosystems of the US Midwest near Indianapolis, IN. For the 8 storms analyzed, results showed that bulk precipitation amount was the best predictor of mean and maximum tile flow, time to peak and runoff ratio. The contribution of macropore flow to total flow increased with precipitation amount, representing between 11% and 50% of total drain flow, with peak contributions between 15% and 74% of flow. For large storms (> 6 cm rainfall), cations data indicated a dilution of groundwater with new water as discharge peaked. Although no clear indication of dilution was observed for

smaller storms (< 4 cm rainfall), macropore flow still contributed between 11% and 17% of total flow. For large storms, the transport of dissolved organic carbon (DOC), total phosphorous (TP) and soluble reactive phosphorus (SRP) was found to be regulated mainly by macropore flow while nitrate transport was regulated mainly by matrix flow. For smaller storms, macropore flow dominated DOC and TP transport while SRP and nitrate transport was dominated by matrix flow. These results significantly increase our understanding of the hydrological functioning of tile drained fields and its interaction with N, P and C transport in spring, which is the time of the year during which most water and N losses from tile drains occur in the Midwest.

Philippe G. Vidon, Ph.D., Committee Chair

## TABLE OF CONTENTS

<b>Introduction</b> .....	1
<b>Materials and Methods</b> .....	8
Site Description.....	8
Storm Event Sampling and analysis.....	9
Hydrological measurements and water quality analysis.....	9
Hydrograph Separation .....	12
Data analysis .....	14
Statistical Analysis.....	15
<b>Results</b> .....	17
Storms characteristics and tile drain response.....	17
Hydrograph separation .....	18
Cation Concentration Dynamics .....	20
Nutrient Concentration Dynamics.....	21
Nutrient fluxes and export rates .....	23
<b>Discussion</b> .....	25
Analysis of the error.....	25
How do precipitation characteristics affect tile drain flow response during storms?.....	27
What is the relative importance of matrix flow and macropore flow, as transport pathways, during storms events?.....	29
What is the relative importance of matrix flow and macropore flow in nitrogen, phosphorus and dissolved organic carbon transport to tile flow during storm events?.....	30
How do precipitation characteristics affect nitrogen, phosphorus and carbon fluxes/export rates? .....	35
<b>Conclusions</b> .....	39
<b>Tables</b> .....	41
<b>Figures</b> .....	48
<b>References</b> .....	71
<b>Curriculum Vitae</b>	

## LIST OF TABLES

Table 1. Precipitation characteristics.

Table 2. Hydrological response of the tile drains.

Table 3. Event and pre-event contributions for storms.

Table 4. Correlation between event water and solutes concentrations.

Table 5. Correlations between precipitation characteristics and tile drain response.

Table 6. Fluxes and export rates.

Table 7. Correlation between solute concentrations, precipitation and tile response.

## LIST OF FIGURES

- Figure 1. Study area.
- Figure 2. Aerial view of the study area.
- Figure 3. Cross section of the study area.
- Figure 4. Daily precipitation and discharge.
- Figure 5. Water table depth from wells.
- Figure 6. Percent of new water and discharge.
- Figure 7. Box plots of  $Mg^{2+}$  concentrations.
- Figure 8.  $Mg^{2+}$  concentrations and discharge.
- Figure 9. Box plots of  $K^+$  concentrations.
- Figure 10.  $K^+$  concentrations and discharge.
- Figure 11. Box plots for DOC concentrations.
- Figure 12. DOC concentrations and discharge.
- Figure 13. Box plots for SUVA values.
- Figure 14. SUVA values and discharge.
- Figure 15. Box plots for  $NO_3^-$  concentrations.
- Figure 16.  $NO_3^-$  concentrations and discharge.
- Figure 17. Box plots for  $NH_4^+$ .
- Figure 18.  $NH_4^+$  concentrations and discharge.
- Figure 19. DON concentrations and discharge.
- Figure 20. Box plots for TP concentrations.
- Figure 21. TP concentrations and discharge.
- Figure 22. Box plots for SRP concentrations.
- Figure 23. SRP concentrations and discharge.
- Figure 24. Conceptual model for solute transport.

Figure 25. Bar graph for N species.

Figure 26. Bar graph for P species.

## INTRODUCTION

The development of intensive agriculture and the increase in the use of fertilizers and pesticides in the US Midwest in the last 50 years has caused nitrogen, phosphorus and pesticides losses from agricultural land to streams to greatly increase in many landscapes, including the Mississippi Drainage Basin (MDB). Exports of nitrogen (N), phosphorus (P) and dissolved organic carbon (DOC) have been identified as causes of many water quality problems both locally and nationally and have also been linked to the eutrophication of lakes and coastal waters (e.g., development of large zones of hypoxic bottom waters in the Gulf of Mexico every summer; Goolsby et al., 2000). Characterizing the primary hydrological controls regulating water, DOC, N and P export to streams in agricultural landscapes of the Midwest is therefore critical to the development of successful strategies to improve water quality with respect to nutrients at the watershed scale (Sidle et al., 2000). The United States Environmental Protection agency (USEPA) has identified agriculture as the major nonpoint source of P to surface waters, and the greatest impediment to achieving the water quality goals stated in the Clean Water Act (Gentry et al., 2007). Some authors (Royer et al., 2006; Gentry et al., 2007) have highlighted the importance of addressing water quality issues in the Midwest in order to understand the mechanisms that move nutrients and contaminants from and to Midwestern streams.

Agricultural subsurface drainage, commonly referred to as tile drainage, is a water management practice used in poorly drained soils to facilitate access to and cultivation of agricultural land in humid regions. Subsurface drainage is an important component of successful agricultural water management in areas with shallow ground water (Fox et al.,

2004). However, tile drains have been identified as an important transport pathway for the export of high amount of nutrients and contaminants, from cropland to surface water systems (Fox et al., 2004; Gentry et al., 2007; Kladivko et al., 1991; Kladivko et al., 1999). The discharge of nutrient-rich tile drain water into ditches and streams negatively affects surface water quality and a range of ecological process in receiving water bodies. Understanding the processes controlling the delivery of nutrients to streams in artificially drained landscapes in the Midwest is therefore of paramount importance in order to understand the impact of drainage on water quality.

One hydrological condition that becomes important in artificially drained landscapes is the existence and degree of influence that preferential flow paths (or macropores) have on water flow to tile drains. Macropores are conduits in the soil; created by plant roots, soil cracks or soil fauna. Preferential flow paths make an unsaturated soil behave like a perforated filter (Kung et al., 2000), thus in essence preferential flow through soil macropores results in the rapid movement of nutrients, pesticides and other contaminants from the soil surface to subsurface drains (Kladivko et al., 1999; Kladivko et al., 2001; Stone and Wilson, 2006). This rapid movement is not believed to be caused only by the tensional and gravitational forces that control matrix flow, instead, this behavior has been found to be caused by a small portion of macropores directly connected to the drains (Fox et al., 2004). The role of macropores in tile flow has been previously studied by Stone and Wilson (2006) but little is known about the importance of preferential flow pathways on N, P and C transport in tile drains.

Some authors have associated old water (or pre-event water) discharge with matrix flow and new water (or event water) discharge with macropore flow (Sidle et al.,

2000; Stone and Wilson, 2006). A technique called hydrograph separation is often used to determine the proportion of old water and new water added to a stream. With the use of this technique, Hill and Waddington (1993) found a dominance of pre-event water in streams during storm events. Using the same technique, Stone and Wilson (2006) observed variations in the nutrient transport flow paths at different stages of the storms studied. Baker et al. (2006) suggested that during most storm events, tile drains and macropores are the primary transport pathways for agricultural chemical export in a tile-drained field located in central Indiana. Sidle et al. (2000) found that with an increase in moisture conditions in soils, the spatial interconnections between macropores also increase, increasing its contribution to stormflow generation from < 1% to 15% in some cases.

It is well established that most nutrient export occurs during episodic high flow periods (Kladvko et al., 1999; Kladvko et al., 2001; Inamdar et al., 2004; Royer et al., 2006; Stone and Wilson, 2006). Surface runoff and tile drain flow generally exhibit peak flow rates in response to storm events (Kladvko et al., 2001). Nutrient concentration in streams, hydrological processes and flow paths often change rapidly during precipitation events in response to variations in precipitation intensity/duration and pre-event moisture conditions (Hangen et al., 2001; Inamdar et al., 2004). Several studies have shown that stream DOC concentrations often peak on the rising limb of the snowmelt and rainfall-induced hydrographs, prior to discharge peak, followed by a rapid decrease in concentrations following rainfall cessation or melt decline (Boyer et al., 2007; Hood et al., 2006; Turgeon and Courchesne, 2008).

With the exception of a few recent studies (Dalzell et al., 2005; Royer and David, 2005; Vidon et al., 2008a; Wagner et al., 2009), most studies investigating dissolved organic carbon (DOC) sources and pathways to streams take place in forested mountainous catchments. Similar research is therefore needed in other physiographic regions of the country, especially in artificially drained landscapes of the Midwest where little research has been done on the primary hydrological controls regulating DOC fluxes to streams. It is also highly important to characterize the spectroscopic and chemical signature of DOC since it can provide information about the sources of DOC in stream water and source changes during hydrological events. Weishaar et al. (2003) found that spectroscopic analyses, such as specific UV absorbance (SUVA), have the potential to provide information about shifts in the chemical character of aquatic DOC. They found that SUVA was a good indicator of the humic fraction of DOC and is strongly correlated to its aromaticity, suggesting that shifts in the character of stream water DOC during storm events have the potential to provide information about which source pools of DOC are hydrologically connected to the stream, and/or transformation of DOC along flowpaths to catchment outlets.

It is also important to characterize the temporal and spatial patterns of nitrogen export as they can help in understanding the mechanisms and conditions that affect the movement of nitrogen from different sources to streams. Inamdar et al. (2004) focused their research on the study of temporal and spatial patterns for  $\text{NO}_3^-$  and DOC transport in a forested watershed. They found that  $\text{NO}_3^-$  concentrations peaked early on the rising limb of the hydrograph, suggesting that stream flow  $\text{NO}_3^-$  is derived from till groundwater. The early appearance of  $\text{NO}_3^-$  in the stream flow was attributed to the

displacement of till waters by infiltrating precipitation. Using a combination of isotopic, chemical and hydrometric data, McHale et al. (2002) found that soil water  $\text{NO}_3^-$  concentrations were not greatly affected by changes in antecedent moisture conditions and season. According to end member mixing analysis, soil water and till groundwater dominated both stream base flow and storm flow.

The mechanisms and pathways of P transfer are complex, and while advances in our knowledge have been made, there is still much that is poorly understood or under-investigated. A good example is the lack of long-term intensive data needed to provide a complete understanding of P transport from fields to streams (resulting forms, concentration, and loads) under a range of flow conditions (and controlling weather patterns) in heavily tile-drained agricultural watersheds. Gentry et al. (2007) focused their research on determining the dominant P form (dissolved or particulate) and identifying the primary P transport pathways in a tile-drained agricultural watershed, using intensive long-term data. By closely examining high discharge events in tile flow, they were able to identify extreme discharge events as the source of the majority of annual stream Total Phosphorus (TP) load, as both Soluble Reactive Phosphorus (SRP) and Particulate Phosphorus (PP) concentrations increased with stream discharge, especially during periods with high sediment loads. They also found that tile drains are likely to be major contributors of SRP every year, with variability attributed to seasonality. Royer et al. (2006) focused their research on temporal patterns for riverine exports of  $\text{NO}_3^-$  and phosphorus from agricultural watersheds in Illinois, and the implications for reducing nutrient loading to the Mississippi river. They found that SRP export occurred mainly from January to June in most years, although substantial export occasionally occurred

later in the summer period. Mechanistically, they found that overland flow was important for export of SRP and TP during flooding and high tile discharge periods. In contrast, for dry periods with small P export, nearly all SRP and total P inputs to the river appeared to be from tile drainage.

Beyond specific mechanisms regulating N, P and C export to streams in artificially drained landscapes of the US, a better characterization of  $\text{NO}_3^-$ ,  $\text{NH}_4^+$ , DON, SRP and TP fluxes to stream via tile drains is also important. Indeed, to address nutrient inputs from non point sources, states are currently developing nutrient criteria, numeric standards and total maximum daily loads (TMDLs) for nutrient-impaired streams and rivers. A TMDL represents the maximum load ( $\text{kg d}^{-1}$ ) of a nutrient that a stream can receive and still maintain water quality sufficient to meet its designated uses (Royer et al., 2006). Various studies have focused on long term data to address: the temporal and spatial patterns of nutrients loads and export, the role of hydrology in controlling export and the implications of these patterns for efforts, such as TMDLs, to reduce eutrophication and nutrient export from the Midwest (Royer et al., 2006; Kladivko et al., 2001; Dalzell et al., 2005). But there is a lack of studies that focus on high-resolution short-term nutrient export and fluxes to streams via tile drains, which could be a key factor in understanding and regulating nutrient export from Midwestern tile-drained fields, since most nutrient export occurs in periods of high discharge over a short period of time.

Based on the lack of information related to the role of macropore flow in water and nutrient transport and their interaction with tile drains, especially in the Midwest area, three primary objectives were addressed in this research:

- **Objective #1:** Identify the relative importance of matrix flow and preferential flow through soil macropores to tile flow during storm events in an artificially drained landscape in central Indiana, in the Midwest area of the US.

- **Objective #2:** Identify the relative importance of storm characteristics and preferential flow through soil macropores on nitrogen, phosphorus and carbon transport in tile flow in an artificially drained landscape in central Indiana, in the Midwest area of the US.

- **Objective #3:** Identify the relative importance of storm characteristics on nitrogen, phosphorus and carbon fluxes/export rates in an artificially drained landscape in central Indiana, in the Midwest area of the US.

## MATERIALS AND METHODS

### *Site Description*

The selected area for this study is a 7.2 km<sup>2</sup>, first order watershed, located in Hancock County, Indiana, 32 kilometers east of Indianapolis, and locally known as Leary Weber Ditch (LWD) (Figure 1). Two tile-drain outlets (TD1 and TD2) located in the headwater of the watershed (Figure 2) were monitored at this site, which is on an active, private farm that uses a corn and soybean crop rotation under conventional tillage. Each tile drain is 20.3 cm internal diameter (ID) and located approximately 120 cm below ground surface. TD1 extends 660 m from the stream and drains an area approximately 8.1 ha in size. TD2 extends 710 m from the stream and drains an area approximately 6.1 ha in size. The drainage area of each tile drain was calculated with the help of the map presented in Figure 2, which was the only available description of the location and length of the tile drainage system in LWD.

The climate at the site is classified as temperate continental and humid. The average annual temperature for the central Indiana area is 11.7°C with an average January temperature of -3.0°C and an average July temperature of 23.7°C. The long term average annual precipitation (1971-2000) is 100 cm (NOAA, 2005). May is the wettest month of the year with average rainfall of 25 to 28 cm and February is the driest month of the year statewide (Indiana State Climate Office, 2009). Soils in LWD are suited for row crop agriculture, such as corn and soybean, but require artificial drainage to lower the water table, remove ponded water, and ensure good soil tilth.

The area is dominated by poorly drained soils and a nearly flat surface topography. Soils in LWD watershed include the Crosby-Brookston soil association (fine,

mixed, active, mesic Aeric Epiaqualfs and fine-loamy, mixed, super active mesic Typic Argiaquolls) (Stone and Wilson, 2006). Soils in this association are characterized by a high water-holding capacity and a poor drainage characteristic (Kladivko et al., 1999). These soils contain high amounts of clay and organic-matter, and may have a higher tendency for the formation of preferential flow paths than coarse-textured and poorly structured soils (Stone and Wilson, 2006).

Agriculture is the principal land use, with 87% of the total area in row crops (Baker et al., 2006). Conventional tillage and a corn/soybean rotation has been implemented consistently for the last 20 years at LWD watershed. LWD is an intermittent stream and a tributary to Sugar Creek. The ditch has been dredged along much of its reach to facilitate drainage of the shallow water table. Successful farming requires lowering the water table and removing ponded water by artificially draining the fields through tiles. Tile drains are the primary transport pathways for agricultural-chemical transport to LWD during most storms as well as between storms (Baker et al., 2006; Baker et al., 2007).

### *Storm Event Sampling and analysis*

#### Hydrological measurements and water quality analysis

Event sampling was conducted between May and June 2008. A total of 8 storms large enough to generate tile flow occurred during this time interval. Precipitation timing and intensity was monitored continuously at 15-minute intervals by a Vaisala WXT510 Multi-Parameter Transmitter weather station located 500 m from the tile-drain outlets. Additionally, four graduated rain gauges were deployed 5 m from tile-drain outlets to

capture precipitation chemistry and variability in bulk precipitation. Each of the tile drains (TD1 and TD2) was equipped with a Doppler velocity meter (Teledyne Isco 2150 open channel flow-meter) for discharge measurements, set at a 15-minute interval. TD1 and TD2 were also equipped with an In-Situ LTC probe to monitor water level, temperature and electrical conductivity at a 15 minute-interval. Two groundwater wells (5.4 cm ID, 2 m deep) were installed near the edge of the field where TD1 and TD2 were located and equipped with continuous water level loggers (YSI 600 XLM) to monitor water table response to storms in relation to tile flow for the storms studied. Well 1 was located approximately 5 meters from TD1 and Well 2 at the inter-drain line immediately downstream from TD1 (Figure 2).

Water samples for water quality analysis were collected for four storms in TD1 and two storms in TD2. Two ISCO 6712 auto samplers were deployed in each tile-drain outlet, respectively, to collect high resolution water samples during the events. The samples were collected in Teledyne ISCO ProPak® sample bags, made of EPA-approved low density polyethylene (LDPE) plastic. The sample collection line from each ISCO sampler was located at least 1 m into the tile drains. Doppler velocity meter measurements were used to identify any flow reversals that could occur when the tile drain outlets were submerged. Each sampler was triggered manually before the beginning of each storm and programmed to collect water samples every 20 minutes during the rising limb of the hydrograph. Each 900 mL sample was a composite of three 300 mL samples taken 20 minutes apart. The sampling interval was extended to 2 hours (three water samples taken 40 minutes apart per bottle) during the falling limb of the hydrograph. Samples were never left more than 24 hours in the field.

All water samples (tile-drain water and precipitation) were analyzed for specific electrical conductivity (EC) using a benchtop EC meter (Oakton CON 510) upon return to the laboratory and filtered using GF/F Whatman 0.7  $\mu\text{m}$  filters (except for samples preserved for TP analysis). The water samples were analyzed for nitrogen (TDN,  $\text{NO}_3^-$ ,  $\text{NH}_4^+$ ), phosphorus (TP, SRP), DOC and SUVA. DOC and TDN concentrations were determined using a Shimadzu TOC 4110 On-line TOC analyzer at the Environmental Chemistry research laboratory at Indiana University (Bloomington, IN).  $\text{NO}_3^-$ ,  $\text{NH}_4^+$  and SRP concentrations were determined using a Konelab 20 Photometric analyzer (EST Analytical) by the Hydrazine Reduction method (EPA method 353.1), EPA method 350.1 and the ascorbic acid method (EPA method 365.2), respectively. TP concentrations were determined colorimetrically post-digestion with persulfate and  $\text{H}_2\text{SO}_4$  (SM 4500-P) with the Konelab 20 Photometric analyzer (EST Analytical). Samples were also analyzed for chloride, major cation concentrations ( $\text{Ca}^{2+}$ ,  $\text{K}^+$ ,  $\text{Mg}^{2+}$  and  $\text{Na}^+$ ) and oxygen-18 isotope of water.

Chloride concentrations were determined by colorimetry (EPA method 325.2) using a Konelab 20 Photometric analyzer (EST Analytical). Major cation concentrations were determined using an ion chromatograph (Dionex DX500) and a CS15 analytical column and methasulfonic acid eluent at University of North Carolina-Charlotte. Five milliliter aliquots of all samples were analyzed for oxygen-18 of water using equilibration with  $\text{CO}_2$ , in the Stable Isotope Research Facility at Indiana University in Bloomington, IN using a ThermoFinnigan Gas Bench inlet interfaced with a Delta Plus XP isotope ratio mass spectrometer. The natural abundance of oxygen-18 isotope of water is expressed in

$\delta$  (per mil) ratio of the sample to the Vienna Standard Mean Ocean Water (VSMOW) standard where R is the ratio of  $O^{18}/O^{16}$  (Liu et al., 2004):

$$\delta O^{18}_{\text{sample}} = [ (R_{\text{sample}} / R_{\text{VSMOW}}) - 1 ] \times 10^3 \quad (1)$$

### *Hydrograph Separation*

Hydrological tracers (cations, oxygen-18) were used to differentiate the relative contribution of new water (event water) and old water (pre-event water) to the stream during each storm, and to differentiate the relative importance of new water and old water in tile drain flow. A two component isotopic separation was used to separate stormflow into pre-event water and event water on the basis of the stable isotope ratios or EC of each component. This model uses a combination of mass balance equations for water and tracer fluxes in the form:

$$Q_t = Q_p + Q_e \quad (2)$$

$$Q_t C_t = Q_p C_p + Q_e C_e \quad (3)$$

where Q is discharge, C is  $\delta^{18}O$  composition of water or EC; t represents the total stream flow; p and e represent pre-event and event components, respectively. Relative contributions of event and pre-event water were calculated for each tileflow sample collected. The isotopic composition (or EC) of baseflow represented the pre-event component while the isotopic composition (or EC) of the rain sample represented the event component (Brown et al., 1999).

Two of the major assumptions that this method involves state that (1) storm tileflow is supplied only by two water types, pre-event water and event water, each having spatially and temporally uniform isotopic values which are significantly different; and (2) surface water storage contributions are considered either negligible during storms

or to have similar isotopic signature as groundwater. In view of the errors which may arise in hydrograph separation, it is important to evaluate these assumptions (Hill and Waddington, 1993). Although oxygen-18 and EC were the primary tracers used in this study for hydrograph separation, cations and chloride were also used as appropriate to provide an independent estimate of the relative importance of new/old water to tile flow. In 2006, Stone and Wilson used tile drain flow, major ion chemistry and specific conductance data to support the idea that the major ion chemistry of water moving through preferential flow was different from that of matrix flow. They calculated the Spearman  $\rho$  correlation coefficients for tile drain flow and specific conductance in relation to the major ions. A strong positive correlation was found between specific conductance and chloride. They also found a strong negative correlation between specific conductance and tile drain flow, and between chloride and tile drain flow. These correlations suggested that lower ionic-strength water from the field surface contributed to the tile drain flow at an increasing rate as the tile flow increased. There were no surface inlets to this tile-drain; therefore the lower ionic-strength water likely reached the tile drain by preferential flow. Matrix flow cannot account for the rapid movement of the low ionic-strength water that reached tileflow within hours from the onset of precipitation; therefore macropores are believed to be the main transport pathway to tileflow. Based on this analysis, old water was considered to reach the tile flow through matrix flow and new water was considered to reach the tile flow through macropore flow. Water flowing through soil macropores during storms has very little contact with the soil matrix and therefore generally maintains a chemical and isotopic signature similar to that of precipitation water (Stone and Wilson, 2006).

### *Data analysis*

In this study, the start of each event was defined when a perceptible rise in discharge in the tile-drain outlet was observed. The end of the event was defined when tile flow returned to pre-event flow values. Seven-day and thirty-day antecedent precipitation for each event were calculated by computing total precipitation (cm) in the seven and thirty days preceding the events using weather station data, respectively. The runoff ratio for each storm is the ratio of total tile discharge for the event expressed in centimeter (discharge normalized by area) divided by the bulk precipitation for the event, also expressed in centimeter. The hydrograph response time is defined as the time between the beginning of precipitation and the beginning of a perceptible increase in discharge. The time to peak is defined as the time between the start of the rising limb and the peak in discharge (Poor and McDonnell, 2007).

Changes in DOC and in each N and P species during the storms were characterized in order to 1) identify the relative importance of each water delivery pathway to N, P and C exports during storms, and 2) determine changes in the nature of N, P and C along each of these pathways as the storm progressed. The main variables analyzed were: loads, fluxes and maximum, minimum and average concentrations of DOC, DON, TDN,  $\text{NO}_3^-$ ,  $\text{NH}_4^+$ , TP and SRP; timing for DOC to peak (defined as the period of time between the start of each event and the maximum observed DOC concentration) and timing for  $\text{NO}_3^-$  maximum dilution (defined as the period of time between the start of each event and the minimum observed  $\text{NO}_3^-$  concentration). DON concentrations were calculated by subtracting  $\text{NO}_3^-$  and  $\text{NH}_4^+$  concentrations from TDN concentrations ( $\text{DON} = \text{TDN} - \text{NO}_3^- - \text{NH}_4^+$ ). Whenever  $\text{NO}_3^- + \text{NH}_4^+$  value was greater

than TDN (due to instrument uncertainty), DON was reported as zero. The Specific UV Absorbance of DOC (SUVA) was also measured for each DOC sample and used as an indicator of the aromaticity of DOC. It was also used to determine the relative abundance of humic/non-humic substances in DOC (Weishaar et al., 2003; Hood et al., 2006). DOC, DON, TDN,  $\text{NO}_3^-$ ,  $\text{NH}_4^+$ , TP and SRP fluxes (g/h) were calculated by multiplying the flow rate value by the respective average nutrient concentrations at each sampling point. The total fluxes (g/storm) represent the sum of all the hourly fluxes for each nutrient per storm. Export rates (kg/ha/storm) for each nutrient were calculated by dividing the total fluxes, previously calculated, by the tile-drain drainage area.

### *Statistical Analysis*

SigmaPlot 11.0 was used for statistical analysis. Storm characteristics for storms 1-8 (bulk precipitation, rain intensity, maximum intensity, duration of the storm and 7-day antecedent precipitation) and tile drain response to storms 1-8 (mean tile flow, maximum tile flow, hydrograph response time, time to peak and runoff ratio) were tested for normality and equal variance. T-tests were used to determine significant differences between these two groups if normally distributed. Significance levels of differences between non-normally distributed data were determined using Mann-Whitney Rank Sum Tests. The same procedure was used to evaluate the percentage of new water added to tile flow per storm (S2, S5, S6 and S8 for TD1 and S5 and S8 for TD2) vs. DOC, TP, SRP  $\text{NH}_4^+$ ,  $\text{NH}_3^-$  and DON average concentration per storm (S2, S5, S6 and S8 for TD1 and S5 and S8 for TD2). If normally distributed, t-tests were used to determine significant differences between mean tile flow and bulk precipitation, and DOC, TP, SRP  $\text{NH}_4^+$ ,

$\text{NH}_3^-$ , DON average concentration per storm (S2, S5, S6 and S8 for TD1 and S5 and S8 for TD2). Mann-Whitney Rank Sum Tests were used to determine significance levels of differences between these data if non-normally distributed.

## RESULTS

### *Storms characteristics and tile drain response*

Eight storm events were large enough to generate/increase tile flow in TD1 and TD2 between April and June 2008 (Figure 4). During the month of April, the total precipitation amount was 57% below average, while May and June were above average (27% and 76%, respectively), according to the NOAA 1971-2000 monthly climate averages (NOAA, 2009). The bulk precipitation for the events studied was between 2.2 cm and 3.8 cm, with the exception of storms 5 and 6 during which total precipitation was 6 cm or higher (Figure 4). Antecedent moisture conditions varied widely during the study period. For storms 1-5, the average 7-day antecedent precipitation was 4.28 cm while for storms 6-8 the 7-day antecedent precipitation was 14.68 cm (Table 1). Thirty-day antecedent precipitation was not available for storms 1-3, but it consistently increased from storm 4 (14.2 cm) to storm 8 (37.38 cm) (Table 1).

Before the onset of precipitation, tile drains were generally not flowing (baseflow  $\approx 0$ ) (Table 2). Mean and maximum tile flow were highest for storms 5 and 6 for both tile drains with mean tile flow above 36 L/s for TD1 and above 14 L/s for TD2. Maximum and mean tile flows were higher for TD1 (average 43 L/s) than for TD2 (average 21 L/s). Both tile drains showed extremely variable response times from storm to storm, ranging from 15 min to 400 min. The time to peak was also variable for the different storms studied, ranging from 15-30 min to 360 min for TD1 and 855 min for TD2 (storm 6). Tile flow in TD1 was generally slightly higher than flow in TD2 for storms 2, 3, 4, 7 and 8 and higher than TD2 for storms 5 and 6 (Figure 5). The runoff ratio was also variable from storm to storm, but it progressively increased during the

course of the study (Table 2). The lowest runoff ratios were reported during storms 1 and 2 and ranged from 0.04 to 0.22. The highest runoff ratios in TD1 were observed during storms 5 and 6 with a value of 0.70. The highest runoff ratios for TD2 were observed during storms 5 and 8 (0.39 and 0.45, respectively).

Water table response to precipitation was recorded in wells 1 and 2, and was analyzed in relation to TD1 because of its proximity to well 1 (5 m) and well 2 (15 m) (Figure 5). During the months of April 2008 and June 2008 the average water table depth was 1.54 m below ground surface (BGS) before the onset of precipitation and rose by an average of 18 cm in well 1 and 22 cm in well 2 during the storm events studied. Storm 6 showed the highest water table level (0.82 m BGS in well 1 and 1.04 m BGS in well 2). The timing of the water table rise in relation to discharge varied among the different storms. For storms 2, 5 and 6 the water table peaked shortly before or during the peak in discharge while for storms 1, 3, 4, 7 and 8 the water table peaked after the peak in discharge.

#### *Hydrograph separation*

Specific electrical conductivity (EC) of precipitation for storms 2, 5, 6 and 8 ranged from 5.63  $\mu\text{S}/\text{cm}$  to 31.9  $\mu\text{S}/\text{cm}$  at 20°C, while baseflow EC values before each storm studied ranged from 452  $\mu\text{S}/\text{cm}$  to 490  $\mu\text{S}/\text{cm}$ . The oxygen-18 signature of water in tile flow before each storm varied from -7.03‰ for storm 2 to -6.63‰ for storm 8 (Table 3). However, the oxygen-18 signature of precipitation water and baseflow tile water were not sufficiently different to allow the completion of a hydrograph separation for storms 5 and 6. Based on the hydrograph separation conducted with EC, total tile flow

contributions of new water were highest for storms 5 and 6 (43% to 50% new water) and lowest for storms 2 and 8 (11% to 17% new water) regardless of the tile drain investigated (TD1 or TD2). Maximum contributions of new water during the storms studied were also highest for storms 5 and 6 (63% to 74% new water) and lowest for storms 2 and 8 (15% to 33% new water) regardless of the tile drain. When available, results from the hydrograph separations conducted using oxygen-18 indicated overall contributions of new water to total flow 11% higher than with the hydrograph separation based on EC (average of 3 available values). Maximum contribution of new water during storms 2 and 8, as calculated using oxygen-18, was 20% higher than with the EC method (average of 3 available values). Although the proportion of new water estimated using the oxygen-18 based hydrograph separation indicated a higher proportion of new water in tile flow than the EC based hydrograph separation method, the patterns of new water contributions during the storms for which both methods were used (i.e. storms 2 and 8) were similar to each other (data not shown). For storms 5 and 6, a sharp increase in new water contribution was observed as discharge increased in both TD1 and TD2; however, as the volume of new water (L/s) decreased on the falling limb of the tile hydrograph, the proportion of new water (% total flow) remained high until stream flow returned almost to baseflow condition. This pattern was especially clear during storm 5 in TD1 and TD2 where an abrupt decrease in the proportion of new water in total flow was observed as flow returned to pre-storm level (Figure 6).

For the smaller storms which did not generate discharges above 20 L/s (storms 2 and 8), no clear and consistent patterns of new water contribution were observed. For storm 2, the volume of new water increased with flow, but the maximum proportion of

new water in total flow occurred on the rising limb of the hydrograph. For storm 8, in both TD1 and TD2, the volume of new water and the proportion of new water in total flow both increased and decreased with flow, but showed no response to changes in total flow compared to the other storms.

### *Cation Concentration Dynamics*

Figure 7 shows box plots of  $Mg^{2+}$  concentrations (minimum, mean, lower quartile, upper quartile, maximum). Maximum concentrations ranged from 15.88 mg/L to 18.15 mg/L and average concentrations ranged from 8.87 mg/L to 13.79 mg/L.  $Mg^{2+}$  concentrations showed a larger variability during storms 5 and 6 (from  $\approx 4$  mg/L to 16 mg/L) than during storms 2 and 8 (from  $\approx 10$  mg/L to 15 mg/L). Figure 8 shows  $Mg^{2+}$  concentration patterns for storms 2, 5, 6 and 8 in TD1 and for storms 5 and 8 in TD2. For storms 5 and 6 (which generated discharge  $> 30$  L/s in TD1 and TD2) a clear dilution pattern can be observed for  $Mg^{2+}$  with minimum concentrations between 5-10 mg/L, observed during or immediately after the peak in discharge. No clear increase in concentrations or dilution patterns were observed for  $Mg^{2+}$  concentrations in storms 2 and 8 and the values remained between 10-15 mg/L during most of the storm event. Figure 9 shows box plots of  $K^+$  concentrations, indicating larger variability for storms 5 and 6 than for storms 2 and 8. Maximum  $K^+$  concentrations ranged from 0.44 mg/L to 0.92 mg/L and average concentrations ranged from 0.20 mg/L to 0.40 mg/L. Figure 10 shows  $K^+$  concentrations patterns for storms 2, 5, 6 and 8 in TD1 and TD2. For storms 5 and 6, a clear increase in  $K^+$  concentrations can be observed, with maximum values reached immediately after the peak in discharge for TD1 (storms 5 and 6) and during the peak in

discharge for TD2 (storm 5). No clear pattern could be identified for  $\text{Ca}^{2+}$  and  $\text{Na}^+$  concentrations (data not shown).

### *Nutrient Concentration Dynamics*

Baseflow values for DOC were consistent through the different storms studied, ranging from 2.29 mg/L to 3.64 mg/L. Figure 11 shows DOC concentrations box plots with DOC average concentrations ranging from 3.34 mg/L to 5.96 mg/L. Storms 5 and 6 showed more variation in the concentrations of DOC (from  $\approx 3$  mg/L to 9 mg/L) than storms 2 and 8 (from  $\approx 3$  mg/L to 5 mg/L) (Figure 11). Figure 12 shows DOC concentrations patterns for storms 2, 5, 6 and 8 in TD1 and for storms 5 and 8 in TD2. For storms 2, 5, 6 and 8, a clear increase in DOC concentrations can be observed reaching maximum concentrations immediately after the peak in discharge for storms 5 and 6 (discharge  $> 40$  L/s) and before or during the peak in discharge for storms 2 and 8 (discharge  $< 20$  m/L). Maximum DOC concentration ranged from 9.32 mg/L to 10.20 mg/L for storms 5 and 6; and from 5.83 mg/L to 6.41 mg/L for storms 2 and 8. DOC concentrations were consistently higher on the recession limb than during the rising limb of the hydrograph for all the storms with the exception of TD2 during storm 5. Concentrations dropped faster during storms 5 and 6 than during storms 2 and 8. SUVA analyses were performed to the water samples from storms 2, 5, 6 and 8 (Figure 14). No clear pattern with respect to discharge could be identified from the results.

For  $\text{NO}_3\text{-N}$ , a dilution pattern (decrease in concentration) could be observed as discharge increased during storms 5 and 6 (discharge  $> 30$  L/s). For these two storms, the maximum dilution values were observed during the peak in discharge averaging 2.58

mg/L (Figures 15 and 16). The box plots in Figure 15 do not show a large inter-storm variability in  $\text{NO}_3^-$  concentrations. Mean concentration values ranged from 5.80 mg/L to 7.0 mg/L. For storms 2 and 8 (discharge < 20 L/s) no pattern could be identified with respect to discharge. Mean concentration values ranged from 5.90 mg/L to 7.30 mg/L and minimum concentrations averaged 2.60 mg/L. Figure 17 shows box plots of  $\text{NH}_4^+$ -N concentrations for storms 2, 5, 6 and 8. The box plots in Figure 17 do not show large inter-storms variability in  $\text{NH}_4^+$ -N concentrations.  $\text{NH}_4^+$ -N exhibited a variable pattern with respect to discharge during storms 5 and 6 (Figure 18). During storm 5, TD1 showed a dilution pattern, reaching minimum concentrations of 0.07 mg/L during the peak in discharge.  $\text{NH}_4^+$ -N concentrations in TD2 showed no clear pattern, with an average concentration of 0.18 mg/L (Figure 17). The same behavior was observed for TD1 during storm 6, where no clear pattern could be identified and the average concentration was 0.17 mg/L. Storm 2 showed steady  $\text{NH}_4^+$ -N concentrations around 0.06 mg/L and Storm 8 showed a dilution pattern for TD1 (minimum concentration of 0.09 mg/L) but no pattern with respect to discharge for TD2 (average concentration 0.16 mg/L). DON concentrations did not exhibit any patterns with respect to discharge and the concentrations remained very low throughout the different stages of the storms, with the exception of storm 2, where a dilution pattern could be observed, reaching minimum concentrations before the peak in discharge (Figure 19). DON concentrations for storm 2 ranged from 2 mg/L to 19 mg/L. For TP, an increase in the concentration values can be observed in Figure 21 for storms 2, 5, 6 and 8 following discharge patterns. Storms 5 and 6 (discharge > 30 L/s) showed maximum TP concentrations higher than 0.20 mg/L, slightly delayed with respect to discharge (Figures 20 and 21). Figure 20 also showed

large variability in TP concentrations for storms 5 and 6 than for storms 2 and 8. For storms 2 and 8 (discharge < 10 L/s) maximum TP concentrations were lower than 0.13 mg/L and the peaks could be observed during the maximum discharge period, with the exception of storm 2, where the maximum concentration value was recorded before the peak in discharge. For storms 5 and 6, an increase in SRP concentrations with respect to discharge could be observed (Figure 23). Maximum concentrations ranged from 0.035 mg/L to 0.075 mg/L. These two storms showed larger variability in SRP concentrations than storms 2 and 8 (Figure 22). Maximum concentration values were reached immediately before or during the peak in discharge. The average SRP concentrations during these storms ranged from 0.014 mg/L to 0.021 mg/L. During storm 2, no pattern could be identified with respect to discharge for SRP with an average concentration of 0.012 mg/L. For storm 8, the increase in SRP concentrations followed discharge, reaching maximum concentrations of 0.013 mg/L and 0.019 mg/L for TD1 and TD2, respectively, during the peak in discharge.

#### *Nutrient fluxes and export rates*

Nutrient fluxes and export rates were, in general, higher for storms 5 and 6 (discharge > 40 L/s) than for storms 2 and 8 (discharge < 20 L/s). In the case of DOC total fluxes and export rates, these differences were of two orders of magnitude with values ranging from 12 kg/storm to 40.9 kg/storm during storms 5 and 6, and from 0.7 kg/storm to 4.6 kg/storm for storms 2 and 8. DOC export rates ranged from 1.981 kg/ha/storm to 5.000 kg/ha/storm for storms 5 and 6 and from 0.090 kg/ha/storm to 0.600 kg/ha/storm for storms 2 and 8 (Table 6).  $\text{NO}_3^-$  total fluxes for the two larger storms

(storms 5 and 6) ranged from 9.7 kg/storm to 16 kg/storm with export rates ranging from 1.6 kg/ha/storm to 2 kg/ha/storm (Table 6). For storms 2 and 8,  $\text{NO}_3^-$  total fluxes ranged from 0.8 kg/storm to 6 kg/storm and export rates ranged from 0.1 kg/ha/storm to 0.9 kg/ha/storm (Table 6). For storms 5 and 6,  $\text{NH}_4^+$  export rates ranged from 0.05 kg/ha/storm to 0.1 kg/ha/storm and the total fluxes varied from 320 g/storm to 0.9 kg/storm (Table 6). For storm 2 and 8,  $\text{NH}_4^+$  export rates ranged from 0.001 kg/ha/storm to 0.02 kg/ha/storm while the total fluxes were between 0.006 kg/storm and 0.014 kg/storm (Table 6). DON export rates remained relatively constant throughout the study, ranging from 0.04 kg/ha/storm to 0.3 kg/ha/storm while total DON fluxes varied from 0.3 kg/storm to 2.8 kg/storm (Table 6). In the case of TP, export rates were higher for storms 5 and 6, ranging from 0.04 kg/ha/storm to 0.09 kg/ha/storm, and lower for storms 2 and 8, ranging from 0.001 kg/ha/storm to 0.007 kg/ha/storm. Total TP fluxes varied from 0.008 kg/storm to 0.058 kg/storm (Table 6). SRP total fluxes ranged from 0.004 kg/storm to 0.002 kg/storm and export rates varied from 0.007 kg/ha/storm to 0.02 kg/ha/storm for storms 5 and 6 (Table 6). For storms 2 and 8, total SRP fluxes ranged from 0.0008 kg/storm to 0.007 kg/storm while export rates were very low ranging from 0 kg/ha/storm to 0.001 kg/ha/storm (Table 6).

## DISCUSSION

### *Analysis of the error*

Discharge measurements from the Doppler velocity meters were validated by hand using the bucket method whenever possible (stream water level below tile drain). These analysis indicated that the standard error on the reported Doppler velocity meter measurements was approximately less than 20% for all the storms studied. However, these standard error should be taken into consideration when analysing the accuracy of the fluxes and export rates values reported in the results section. Doppler velocity meter measurements also confirmed that no flow reversals occurred in the tile drains during the storms studied, therefore ensuring that tile samples were not contaminated by streamwater when tiles were submerged during storms.

Triplicate analysis of 10% of all samples and analysis of check standards every 10 samples were performed to assess error measurement, and check for accuracy and precision of measurement techniques. Triplicate analysis indicated that standard error on reported solute values was typically less than 10% for all the solutes analyzed, suggesting that trends reported in this study (or the lack thereof) were not artifacts of measurement errors.

For the hydrograph separation, two methods were used to determine the relative importance of macropore flow and matrix flow in tile flow during storm events (i.e. EC and Oxygen-18 based methods). Although the EC based method slightly underestimated the proportion of new water reaching the tiles during storms compared to the Oxygen-18 based method, patterns of new water contributions were consistent between both methods. The underestimation of the proportion of new water while using the EC based

method is believed to be caused by the fact that while the water is being transported through the soil to tile flow, it is in contact with soil particles which modifies its original ionic content. The isotopic signature of precipitation water has a very low rate of change over small periods of time, and it remains almost constant while being transported through the soil to tile flow. Based on these differences, the Oxygen-18 based method is believed to be more accurate than the EC based method. It is difficult to determine the absolute error on the hydrograph separation; therefore the absolute values reported in the previous section regarding the relative importance of macropore flow vs. matrix flow should be interpreted with caution. Nevertheless, these values were consistent with those found by Stone and Wilson (2006) in LWD, where the authors showed that macropore flow contributions varied between 11% and 51% of total storm tile-drain flow and increased with storm intensity. It is however more expensive and more time consuming to implement than the EC based method. In this study both methods were used together to minimize costs while increasing the accuracy and precision of results.

Although clear inter-storms variations in solute concentrations were observed between storms, concentrations were generally not significantly different between TD1 and TD2 for storms 5 and 8 (only storms with water quality data available for both TD1 and TD2). This suggested that in spite of differences in tile-flow response to precipitation between TD1 and TD2 (Table 1), there was no clear difference in water quality between tile-drains. This is consistent with TD1 and TD2 being adjacent tile-drains; however, the differences in hydrological responses between TD1 and TD2 (especially for large storms, Table 1 and Figure 4) suggest that duplicate or triplicate tile-drain experiments are necessary in order to properly estimate solute fluxes as large flow differences can be

observed between tiles. It is unclear at this point why such large differences in flow characteristics are observed between tiles (especially for large storm events) as no differences in surface water ponding after storms were observed between TD1 and TD2. It is possible that unmapped differences in soil characteristics or slight differences in tile-drain slopes may cause these differences in tile-flow response to precipitation.

*How do precipitation characteristics affect tile drain flow response during storms?*

Precipitation characteristics (amount and intensity) and antecedent moisture conditions have been shown to influence the response of watersheds and stream flows to precipitation events (Sidle et al., 2000; Poor and McDonnell, 2007; Vidon et al., 2009). These studies typically indicated that as precipitation amount/intensity and antecedent moisture conditions increased watersheds generally became more responsive to precipitation events and that runoff ratios typically increased. Although stream flow is different from tile flow, the results presented in the previous sections were consistent with findings observed in streams.

Bulk precipitation appeared to be the most important precipitation characteristic linking tile flow response (mean and maximum tile flow, time to peak and runoff ratio) to precipitation events. During the course of the study, bulk precipitation showed significant relationships ( $P < 0.05$ ) with several hydrological parameters, including mean tile flow, maximum tile flow, time to peak and runoff ratio (Table 5). Maximum precipitation intensity was inversely correlated ( $P < 0.01$ ) to the hydrograph response time, indicating that as the intensity of precipitation increases, the tile flow response time decreases. Although bulk precipitation was not significantly smaller, seven-day antecedent

precipitation and runoff ratio were much lower for storms 1 and 2 than for any other storm, suggesting that drier antecedent moisture conditions could have a significant role in determining tile flow response to precipitation. These results are consistent with the work of Sidle et al. (2000) who, in a steep forested watershed in Japan, documented higher soil connectivity as antecedent soil moisture increased. At a smaller scale, the results presented in the previous section suggest that the same process can be invoked to explain the parallel increase in macropore contribution and antecedent soil moisture observed in the present study.

This study was conducted during a time of the year during which water demand in the soybean field was limited, compared to summer. By the end of the sampling season (mid-June), soybean stems were only 10-15 cm high with an average of three leaves per plant. Since corn presents a much higher water demand earlier in the season, these results might not be applicable to Midwest cornfields. The increase in evapotranspiration and higher crop water demand during late summer might affect the transferability of these results. In a nearby watershed, Vidon et al. (2009), indicated that one spring storm (May 25, 2007) and one late summer storm (Aug. 28, 2007) with similar amount of precipitation (3.6 cm) generated extremely different stream responses to precipitation with a maximum flow of 1,500 L/s for the May storm and 8 L/s for the August storm. These differences in watershed responses were attributed to differences in antecedent soil moisture conditions and crop water demand. The results from Vidon et al. (2009) suggest that the results of the present study might be only applicable to late winter and spring periods during which temperature is moderate and the soil is bare or crop water demand is low. Nevertheless, this is the time of the year that has been identified by Kladivko et al.

(2004) and Royer et al. (2006) as the one with the highest nutrient losses (especially N) to streams via tile drains in artificially drained landscapes of the US Midwest.

*What is the relative importance of matrix flow and macropore flow, as transport pathways, during storms events?*

As discussed in the results section, the total contribution of new water to tile flow ranged from 11% to 50% and maximum contributions ranged from 15% to 74%, depending on the storm. These results were consistent with the findings by Stone and Wilson (2006), who found that for two storms, new water (macropore flow) contributions ranged from 11% to 51% with peak contributions ranging from 40% to 81% with the peaks being consistent with the peak in tile flow. Also consistent with Stone and Wilson (2006), relative contributions of new water to storm flow increased with storm size. For the two largest storms (5 and 6), macropore flow contributions averaged 44% to 50% with peak contributions reaching 70%. For the two smaller storms (2 and 8) macropore flow contributions represented 11% to 17% of total flow, reaching maximum contribution values of 15% to 33% of total storm flow. These results are also consistent with findings by Sidle et al. (2000) who showed that macropore systems increase in importance and may expand during wetter conditions by interacting with surrounding mesopores.

Figures 5 and 6 indicate that for storms 5 and 6, the peak in new water/macropore flow coincides with the peak in discharge and the peak in groundwater contributions. Smaller storms (2 and 8) did not show a clear relationship between water table dynamics and macropore flow contributions. For storm 2, the peak in discharge coincided with the peak in water table while the peak in macropore flow occurred before the maximum

discharge. For storm 8, the relative importance of macropore/matrix flow did not change over the course of the storm and the peak in water table was observed several hours before the peak in discharge. From this result it is possible to infer that the soil response to precipitation events is likely non linear, and that the responses observed for large storms (> 6 cm bulk precipitation) cannot be used as tools to predict the responses of tile flow to smaller precipitation events (< 3 cm bulk precipitation). Cation data support these findings. For storms 5 and 6,  $K^+$  followed the same pattern as discharge and  $Mg^{2+}$  showed a dilution pattern as discharge increased. Previous studies indicated that  $Mg^{2+}$  is typically transported by groundwater flow (most likely to have only soil material and weathering contributions) and dilutions patterns are commonly observed as storm flow discharge increases and gets diluted with precipitation (Hill, 1993; Hood et al., 2006). This is consistent with the hypothesis of the decrease in the relative importance of matrix flow, rich in  $Mg^{2+}$ , as discharge increases during these storms.  $K^+$  is often applied along with other fertilizers to the soil surface in agricultural fields. The increase in  $K^+$  concentrations along with the increase in macropore flow contributions and discharge is therefore consistent with the transfer of surface water, solutes and particles via macropore flow to tile flow. The steady patterns observed for storms 2 and 8 are consistent with the relatively constant contributions of macropore flow to tile flow during these two events.

*What is the relative importance of matrix flow and macropore flow in nitrogen, phosphorus and dissolved organic carbon transport to tile flow during storm events?*

After identifying the storm characteristics that control the tile flow response to storm events and the relative importance of the different transport pathways in the

delivery of new/old water to tile flow during the different storm stages, it is possible to identify the flowpaths regulating N, P and DOC dynamics during precipitation events.

For the two large storms studied (storms 5 and 6), DOC, SRP and TP showed clear increases in concentrations as discharge (and new water contributions) increased. Indeed, the peaks in new water added to tile flow were relatively consistent with the peaks in concentrations of DOC, SRP and TP in tile water. This consistency suggests that macropore flow is the principal regulator of DOC, SRP and TP export to tile flow during the spring season for large storms. In addition, DOC, SRP and TP concentrations followed  $K^+$  concentration patterns; therefore they must be regulated by the same transport mechanism. The percentage of new water added to tile flow during storm events was highly significantly correlated to DOC, SRP and TP concentrations throughout the duration of storm 5, with the exception of TD2 for TP where the values were significantly correlated (Table 4). During storm 6 only DOC was highly significantly correlated to the percentage of new water added to tile flow in TD1 while TP and SRP were significantly correlated to the percentage of new water added to tile flow. These results are consistent with previous studies that have also identified these patterns and linked them to preferential flow through soil macropores as the main transport pathway for DOC, SRP and TP to stream flow during large storm events (Vidon et al., 2008a; Wagner et al., 2008). DOC concentrations typically decrease with depth in the soil profile as the amount of organic matter from plants decreases (McDowell and Wood, 1984; Thurman, 1985), therefore DOC concentrations are low in groundwater and its presence in tile flow water is most likely to be regulated by macropore flow. For the two smaller storms (storms 2 and 8) DOC and TP showed an increase in concentration with respect to discharge,

indicating macropore flow association, while SRP transport was linked to matrix flow. Although for DOC and TP the increase in concentrations followed the same patterns observed for the two larger storms, the maximum concentrations reached during the smaller storms are significantly lower than the maximum concentrations observed for storms 5 and 6. DOC and TP concentrations were highly significantly correlated to the percentage of new water added to tile flow for storms 2 and 8 with the exception of TD1 during storm 8 for TP concentrations. The higher TP concentrations reached during large storms are consistent with the results presented by Gentry et al. (2007), who identified large precipitation events as the source of the majority of annual TP load. DOC concentrations in tileflow (Figures 11 and 12) were consistent with those reported by Wagner et al. (2008). For an agricultural watershed in the Midwest, they found that DOC concentrations varied from 3 mg/L to 11 mg/L during storm events.

Vidon et al. (2008a) studied the DOC specific UV absorbance in their study about changes in the character of DOC in streams during storms in two midwestern watersheds. They found that, for an agricultural watershed, DOC and SUVA quickly increased and decreased with discharge for all storms. These changes in SUVA values suggested that the increase in concentration of DOC in the streams during storms was not simply due to an increased mobilization of a given pool of DOC, but rather to a shift in the dominant source of DOC from mineral soil DOC poor in aromatic substances at baseflow, to near surface soil DOC rich in aromatic substances during storms. The lack of pattern in SUVA values with respect to discharge can be observed in Figure 13. This suggests that for tile flow during the late spring - early summer seasons, there is no clear shift in the source of DOC to tile drains during storms or that the nature of the carbon (SUVA) does not

change as the DOC source changes from deep DOC to surface DOC as suggested by Vidon et al. (2009). Further investigation (soil extractions) is underway to determine whether the SUVA signature of DOC soil extract changes with depth.

During storms 5 and 6,  $\text{NO}_3^-$ -N showed a decrease in concentration, negatively correlated to discharge. For these two storms, the timing of the maximum dilution was consistent with the timing of the maximum new water contributions.  $\text{NO}_3^-$ -N concentrations were inversely correlated to the percentage of new water added to tile flow, with  $\text{NO}_3^-$ -N during storm 6 in TD1 highly significantly inversely correlated and significantly inversely correlated for storm 5 in TD1. These inverse patterns suggest that, for large storms during the spring season,  $\text{NO}_3^-$ -N export to tile flow is mostly regulated by matrix flow. Indeed,  $\text{NO}_3^-$ -N concentrations followed the same  $\text{Mg}^{2+}$  concentrations patterns, suggesting that its transport must be regulated by the same mechanism.  $\text{Mg}^{2+}$  and  $\text{NO}_3^-$ -N concentrations were higher during baseflow (mostly groundwater) than precipitation, indicating pre-event water association. These transport mechanisms were consistent with the N fixation property of legumes, which locates  $\text{NO}_3^-$ -N within the soil matrix. These results were consistent with those from Inamdar et al. (2004), who found that streamflow  $\text{NO}_3^-$ , in a forested watershed, was derived from till groundwater. This behavior was attributed to the displacement of till waters by infiltrating precipitation. Although the concentration patterns described in the previous section and those by Inamdar et al. (2004) were not consistent (mainly because of differences in land uses), the mechanism responsible for  $\text{NO}_3^-$  transport in both cases was similar. For the two smaller storms (2 and 8),  $\text{NO}_3^-$ -N concentrations remained relatively steady and showed no clear patterns with respect to discharge. These patterns were also consistent with those

observed for  $Mg^{2+}$  concentrations, suggesting that  $NO_3^-$ -N and  $Mg^{2+}$  must be exported by the same mechanism. McHale et al. (2002) found that  $NO_3^-$  stream concentrations were not greatly affected by changes in antecedent soil moisture conditions and season; instead,  $NO_3^-$  stream concentrations were regulated by infiltrating precipitation displacing till water. These results were consistent with the observations made for the two smaller storms, which exhibited very different antecedent soil moisture conditions but very similar concentration patterns for  $NO_3^-$ . The dilution pattern with respect to discharge observed for  $NO_3^-$ -N concentrations during storms 5 and 6, and the lack of pattern with respect to discharge during storms 2 and 8 suggests a non-linear response of the soil to storm characteristics for N export.

$NH_4^+$ -N concentrations showed no pattern with respect to discharge throughout the storms studied. The only exception was observed in TD1 during storm 8 where a dilution pattern could be observed with respect to discharge. DON concentrations remained very low throughout the duration of the study and showed no pattern with respect to discharge with the exception of storm 2. During this storm, DON concentrations followed a dilution pattern with respect to discharge.

Overall, data indicate that DOC, TP are most likely to be exported to tileflow through soil macropores, with macropore contributions primarily regulated by bulk precipitation. SRP was found to be transported most likely through soil macropores for large discharge generating events, but no patterns could be identified for smaller events. Data also indicated that  $NO_3^-$ -N is likely to be transported via matrix flow with patterns regulated mostly by storm characteristics. The lack of pattern for  $NH_4^+$ -N and DON concentrations with respect to discharge suggests that their transport is regulated by

contributions from both matrix and macropore flow. Figure 24 shows a conceptual model for nutrient transport regulating mechanisms in tile-drained landscapes of central Indiana. This model was developed based on the results and the discussion presented in the previous sections, and it only applies for the late spring-early summer season, during the early stages of soy bean crops.

*How do precipitation characteristics affect nitrogen, phosphorus and carbon fluxes/export rates?*

Results indicate marked differences in export rates and total fluxes among the storms studied, with the exception of DON export rates and total fluxes which remained relatively constant throughout the study (Table 6). Export rates and fluxes of  $\text{NO}_3^-$ -N,  $\text{NH}_4^+$ -N, SRP, TP and DOC were highest during storms 5 and 6 (consistent with highest flow rates during these storms); and lowest during storms 2 and 8 (Table 6). Indeed, SRP, TP and DOC total fluxes were highly significantly correlated to mean tile flow for storms 2, 5, 6 and 8 (Table 7), while  $\text{NO}_3^-$ -N and  $\text{NH}_4^+$ -N total fluxes were significantly correlated to mean tile flow for storms 2, 5, 6, and 8 (Table 7).  $\text{NH}_4^+$ -N and DOC total fluxes were also highly significantly correlated to bulk precipitation while  $\text{NO}_3^-$ -N, SRP and TP total fluxes were significantly correlated to bulk precipitation for storms 2, 5, 6 and 8. These results were consistent with previous studies (Kladvko et al., 1999; Kladvko et al., 2001; Royer et al., 2006; Stone and Wilson, 2006), which found that periods of high discharge are responsible for the majority of nutrient export from agricultural fields to streams in the Midwest. P and DOC fluxes and export rates from agricultural watersheds have not been well documented. In the literature, there is a

dominance of studies on long-term export rates and fluxes of  $\text{NO}_3^-$ -N from watersheds under different land uses and geographical settings (Randall and Mulla 2001; Kladivko et al., 1999). In 2008, Vidon et al. (b) stressed the importance of accurately estimating contaminant and/or nutrient loading in streams during storms, in order to estimate the impact of various land uses and best management practices on water quality at the watershed scale.

In 2001, Randall and Mulla published a study about  $\text{NO}_3^-$  in surface waters as influenced by climate conditions and agricultural practices. They compiled different studies over annual  $\text{NO}_3^-$  export rates and found large yearly variations related to differences in annual precipitation, crop systems and fertilizer application. For a 6-year period,  $\text{NO}_3^-$  losses varied from 2 kg/ha during the driest year, to 139 kg/ha in a Minnesota tile drained field. These results are consistent with the inter-storm variability for  $\text{NO}_3^-$  export rates reported in Table 6, which were attributed to variations in bulk precipitation. But in the literature, there is a lack of short-term studies on fluxes and per storm export rates, especially in the Midwest area. Only a few authors (Poor and McDonnell; 2007; Vidon et al., 2009) have analyzed these short-term export rates in agricultural watersheds. In 2009, Vidon et al. published a study about seasonal solute dynamics across different land uses. They studied DOC,  $\text{Cl}^-$  and  $\text{NO}_3^-$  (in stream) export rates during 3 storms (one spring storm and two late summer storms), for two watersheds under different land uses (agricultural and mixed land use, respectively). They found that, in the agricultural watershed, DOC and  $\text{NO}_3^-$  export rates varied widely and were higher during the spring season (higher storm flow generation). The differences between storm export rates were in some cases of three orders of magnitude and were linked to the

hydrological response of the watershed to precipitation. During the spring-07 storm (3.6 cm bulk precipitation), in the agricultural watershed, the  $\text{NO}_3^-$  export rate was reported as 0.469 kg/ha/storm and the DOC export rate was reported as 0.551 kg/ha/storm. These results were consistent with the export rate values presented in the previous section (Table 6) for storms 2 and 8 (similar bulk precipitation). For storms 5 and 6, the export rate values presented in Table 6 were three times higher than those reported by Vidon et al. (2009) which is consistent with higher bulk precipitation and mean tile flow reported for these storms.

In 2007, Poor and McDonnell presented their findings about the effects of land use on stream  $\text{NO}_3^-$  dynamics. Their research took place in the Pacific Northwest and studied three different storms from late fall to early spring. They found that, in the agricultural watershed, the  $\text{NO}_3^-$  export rates were very variable, depending on the storm characteristics and antecedent soil moisture conditions. Their overall trends suggested that  $\text{NO}_3^-$  export rates were high during the fall, medium in the winter and low in the spring. For the fall storm (bulk precipitation 2.29 cm) they reported a  $\text{NO}_3^-$  export rate of 0.121 kg/ha/storm, the  $\text{NO}_3^-$  export rate for the winter storm (bulk precipitation 1.67 cm) was 0.040 kg/ha/storm and for the spring storm (bulk precipitation 2.55 cm) the  $\text{NO}_3^-$  export rate reported was 0.021 kg/ha/storm. These export rates are relatively lower than the ones presented in Table 6 in the previous section. The differences in the export rates reported in both studies could be attributed to seasonality and differences in the geographical settings. Poor and McDonnell (2007) conducted their study in the Pacific Northwest. The agricultural watershed studied is described as 50% forested and 50% pasture, with no artificial nitrogen input.

The values reported in Table 6 and Figure 25 for  $\text{NO}_3^-$ -N,  $\text{NH}_4^+$ -N and DON indicated that most of the N exported through tile flow during storm events is mainly  $\text{NO}_3^-$ -N. These contributions were variable during the storms studied, with more than 55% N in the form of  $\text{NO}_3^-$  for storm 2 and more than 85% N in the form of  $\text{NO}_3^-$  for storms 5, 6 and 8. In 2007, Scott et al., published a study about organic nitrogen from headwater streams to large rivers across the conterminous US. They found that for the Northeast and Midwest regions, TON comprised a low percentage (< 20%) of the total riverine nitrogen and that nitrogen export was dominated by  $\text{NO}_3^-$ , which is consistent with the results presented in Figure 24.  $\text{NO}_3^-$  was the dominant N species, with contributions that varied from 55% to 85% (Figure 25) throughout the study.

## CONCLUSIONS

This study investigated the impact of precipitation characteristics on tile flow response to precipitation and the relative importance of macropore flow and matrix flow to tile flow and N, P and C transport at a tile-drained agricultural watershed, representative of the US Midwest. Bulk precipitation amount was found to be the best predictor of mean tile flow, maximum tile flow, time to peak and runoff ratio in spring when vegetation cover was limited and crop water demand was moderate, although some variability in tile flow response could be attributed to antecedent moisture conditions. The contribution of macropore flow to total flow significantly increased with precipitation amount, and macropore flow represented between 11% and 50% of total drain flow, with peak contributions between 15% and 74%. Cations data were consistent with hydrograph separation findings and indicated a dilution of groundwater with new water during the storms as discharge peaked during large storms (> 6 cm bulk precipitation). Macropore flow generally contributed between 11% and 17% of total flow for 2 moderate size storms. These results suggest that the proportion of soil macropores directly contributing to water and solute transport during storms is related to the size of the storm. However, the soil response to precipitation events is likely non linear with variable threshold between large storms (> 6 cm bulk precipitation) and small precipitation events (< 3 cm bulk precipitation), depending on soil type and crop grow stage.

Results showed that DOC and TP concentrations increased with discharge and peaked with maximum contributions of event water, indicating a predominance of macropore flow as transport mechanism. SRP transport was found to be regulated by

macropore flow during large storms (bulk precipitation > 6 cm), but for smaller storms (bulk precipitation < 3 cm) no pattern could be identified, suggesting that matrix flow impacted SRP export for those storms. In general, these three species peaked together for large storms, implying a similar transport mechanism to tile flow.  $\text{NO}_3^-$  showed inverse patterns with respect to discharge, during large storms, indicating a dominance of pre-event water as transport pathway, previously linked to matrix flow.

It is important to keep in mind that these results only apply to the late winter-early spring. High crop water demand and high vegetation cover later in the summer are likely to change the way tile drains respond to precipitation (Vidon et al., 2009). However, late winter-early spring is the period of the year considered to have the most water and N losses from tile drains in the Midwest area of the US (Kladivko et al., 2004, Royer et al., 2006). This detailed storm hydrograph sampling study contributes to the broader understanding of nutrient delivery to tile flow and the hydrological functioning of tile drain systems at a critical time of the year for water quality management. Considering the complexities and variations of tile flow response to precipitation events and the importance of macropore flow to tile flow during storms, it is proposed that more research investigating the variables regulating tile drain hydrology and the relative importance of macropore flow and matrix flow on water and major nutrient/contaminant (e.g. nitrogen, phosphorus, carbon) export to streams over an entire drainage season should be conducted to better inform us on how water, nitrogen, phosphorus and other solute/contaminant exports might change in the future under various climate change scenarios.

TABLES

	<b>Bulk Precipitation (cm)</b>	<b>Maximum Intensity (cm/h)</b>	<b>Average Intensity (cm/h)</b>	<b>Event Duration (h)</b>	<b>7-day antecedent precipitation (cm)</b>	<b>30-day antecedent precipitation (cm)</b>
<b>Storm 1 (May 3)</b>	3.8	9.1	1.5	2.25	3.2	n/a
<b>Storm 2 (May 8)</b>	2.2	1.0	0.19	11.25	7.2	n/a
<b>Storm 3 (May 11)</b>	2.1	1.4	0.15	17.5	3.5	n/a
<b>Storm 4 (May 14)</b>	2.8	1.3	0.16	17	6.0	14.2
<b>Storm 5 (May 30)</b>	7.0	7.9	0.32	21.5	1.6	19.8
<b>Storm 6 (June 4)</b>	10.8	7.1	0.96	10.75	10.6	23.5
<b>Storm 7 (June 7)</b>	2.5	2.8	0.28	8.5	13.4	33.3
<b>Storm 8 (June 10)</b>	2.91	3.9	0.26	11	20.1	37.4

**Table 1:** Precipitation characteristics of storms 1 through 8 from April to June 2008.

	Baseflow (mm/h)		Mean Tile Flow (mm/h)		Maximum Tile Flow (mm/h)		Hydrograph Response Time (min)		Time to Peak (min)		Runoff Ratio	
	TD1	TD2	TD1	TD2	TD1	TD2	TD1	TD2	TD1	TD2	TD1	TD2
<b>Storm 1 (May 3)</b>	0	0	0.24	0.17	0.86	1.22	45	60	15	30	0.04	0.1
<b>Storm 2 (May 8)</b>	0	0	0.29	0.25	0.97	0.76	360	345	105	300	0.11	0.22
<b>Storm 3 (May 11)</b>	0	0	0.71	0.25	1.71	1.15	360	240	45	135	0.36	0.36
<b>Storm 4 (May 14)</b>	0	0.031	0.72	0.44	1.93	1.52	270	255	45	60	0.21	0.3
<b>Storm 5 (May 30)</b>	0	0.002	2.3	0.85	7.2	1.84	15	15	165	405	0.70	0.39
<b>Storm 6 (June 4)</b>	0	0.063	2.65	0.95	7.02	1.94	300	195	360	855	0.70	0.37
<b>Storm 7 (June 7)</b>	0	0.028	0.62	0.5	1.17	0.71	435	405	75	45	0.19	0.26
<b>Storm 8 (June 10)</b>	0	0.039	0.7	0.5	1.24	0.98	90	75	45	30	0.3	0.45

**Table 2:** Hydrological responses of tile drain 1 (TD1) and tile drain 2 (TD2) to precipitation for storms 1 through 8 from April to June 2008.

	<b>Storm 2 TD1</b>	<b>Storm 5 TD1</b>	<b>Storm 5 TD2</b>	<b>Storm 6 TD1</b>	<b>Storm 8 TD1</b>	<b>Storm 8 TD2</b>
<b>Using EC</b>						
Mean New %	17	44	43	50	16	11
Max New %	33	70	63	74	20	15
<b>Using Oxygen-18</b>						
Mean New %	32	-	-	-	21	24
Max New %	47	-	-	-	34	48

**Table 3:** Proportion of new water contribution to tile flow during storms 2, 5, 6 and 8 for tile drain 1 (TD1) and during storms 5 and 8 for tile drain 2 (TD2) using both the specific electrical conductivity (EC) method and the oxygen-18 method. “Mean New %” corresponds to the mean proportion of new water to tile flow over the course of each event. “Max New %” corresponds to the peak contribution of new water to tile flow over the course of each event. Hydrograph separation results using oxygen-18 for storms 5 and 6 are not shown because the isotopic signatures of new and old water were too similar to allow for a hydrograph separation to be conducted using oxygen-18 in water.

	<b>DOC</b>	<b>TP</b>	<b>SRP</b>	<b>NO3</b>	<b>NH4</b>	<b>DON</b>
<b>% NW S2TD1</b>	0.89**	0.88**	-0.35	0.59	-0.31	-0.53
<b>% NW S5TD1</b>	0.85**	0.82**	0.81**	-0.48*	-0.48*	-0.49*
<b>% NW S5TD2</b>	0.89**	0.79*	0.74**	-0.53	-0.45	-0.46
<b>% NW S6TD1</b>	0.62**	0.21	0.35	-0.96**	0.113	-0.29
<b>% NW S8TD1</b>	0.84**	-0.15	0.18	-0.07	-0.72**	0.27
<b>% NW S8TD2</b>	0.77**	0.81**	0.19	-0.18	-0.22	0.06

Significance level: \*\* = 0.01, \* = 0.05

**Table 4:** Pearson correlation coefficients between % of new water added to tile flow (% NW) and dissolved organic carbon (DOC), total phosphorus (TP), soluble reactive phosphorus (SRP), NO<sub>3</sub><sup>-</sup>, NH<sub>4</sub><sup>+</sup> and dissolved organic nitrogen (DON) mean concentrations for storms 2 (S2), 5 (S5), 6 (S6) and 8 (S8) in tile drain 1 (TD1) and 5 (S5) and 8 (S8) in TD2.

	<b>Bulk Precipitation</b>	<b>Maximum Intensity</b>	<b>Average Intensity</b>	<b>Event Duration</b>	<b>7-day antecedent precipitation</b>
<b>Mean Tile Flow</b>	0.74**	0.39	0.07	0.34	-0.03
<b>Maximum Tile Flow</b>	0.68**	0.41	0.11	0.35	-0.19
<b>Hydrograph Response Time</b>	-0.29	-0.72**	-0.41	-0.05	0.16
<b>Time to Peak</b>	0.79**	0.31	0.18	0.15	-0.05
<b>Runoff Ratio</b>	0.56*	0.20	-0.19	0.51*	0.12

Significance level: 0.01 = \*\*, 0.05 = \*

**Table 5:** Pearson correlation coefficients between precipitation characteristics and tile flow responses to precipitation events for both tile drains 1 (TD1) and 2 (TD2) from April to June 2008 (n=16).

<b>Storm 2 TD1</b>	<b>NO<sub>3</sub><sup>-</sup></b>	<b>NH<sub>4</sub><sup>+</sup></b>	<b>DON</b>	<b>SRP</b>	<b>TP</b>	<b>DOC</b>
Total flux (g of X /storm)	800	6.00	700	0.800	8.00	800
Export rate (mg of X /h/m <sup>2</sup> )	1.17	0.01	1.01	0.00	0.01	1.14
Export rate (kg of X/ha/storm)	0.1	0.001	0.08	0	0.001	0.09

<b>Storm 5 TD1</b>	<b>NO<sub>3</sub><sup>-</sup></b>	<b>NH<sub>4</sub><sup>+</sup></b>	<b>DON</b>	<b>SRP</b>	<b>TP</b>	<b>DOC</b>
Total flux (g of X /storm)	16100	600	2800	100	700	31000
Export rate (mg of X /h/m <sup>2</sup> )	6.49	0.24	1.13	0.06	0.27	13
Export rate (kg of X/ha/storm)	2.000	0.07	0.3	0.018	0.080	4

<b>Storm 5 TD2</b>	<b>NO<sub>3</sub><sup>-</sup></b>	<b>NH<sub>4</sub><sup>+</sup></b>	<b>DON</b>	<b>SRP</b>	<b>TP</b>	<b>DOC</b>
Total flux (g of X /storm)	9700	300	400	40	200	12000
Export rate (mg of X /h/m <sup>2</sup> )	5.52	0.18	0.24	0.02	0.14	6.83
Export rate (kg of X/ha/storm)	1.600	0.05	0.07	0.007	0.04	1.900

<b>Storm 6 TD1</b>	<b>NO<sub>3</sub><sup>-</sup></b>	<b>NH<sub>4</sub><sup>+</sup></b>	<b>DON</b>	<b>SRP</b>	<b>TP</b>	<b>DOC</b>
Total flux (g of X /storm)	14200	900	300	100	700	41000
Export rate (mg of X /h/m <sup>2</sup> )	5	0.3	0.1	0.05	0.2	14
Export rate (kg of X/ha/storm)	1.700	0.115	0.040	0.020	0.090	5.000

<b>Storm 8 TD1</b>	<b>NO<sub>3</sub><sup>-</sup></b>	<b>NH<sub>4</sub><sup>+</sup></b>	<b>DON</b>	<b>SRP</b>	<b>TP</b>	<b>DOC</b>
Total flux (g of X /storm)	5900	100	800	6.00	60	4600
Export rate (mg of X /h/m <sup>2</sup> )	3	0.06	0.4	0.00	0.03	2
Export rate (kg of X /ha/storm)	0.700	0.015	0.090	0.001	0.007	0.500

<b>Storm 8 TD2</b>	<b>NO<sub>3</sub><sup>-</sup></b>	<b>NH<sub>4</sub><sup>+</sup></b>	<b>DON</b>	<b>SRP</b>	<b>TP</b>	<b>DOC</b>
Total flux (g of X /storm)	5500	100	1000	7.00	40	3700
Export rate (mg of X /h/m <sup>2</sup> )	3.41	0.09	0.61	0.00	0.03	2.29
Export rate (kg of X /ha/storm)	0.9	0.02	0.2	0.001	0.007	0.6

**Table 6:** Total fluxes and export rates of dissolved organic carbon (DOC), soluble reactive phosphorus (SRP), total phosphorus (TP), NO<sub>3</sub><sup>-</sup>, NH<sub>4</sub><sup>+</sup> and dissolved organic nitrogen (DON) for storms 2 (S2), 5 (S5), 6 (S6) and 8 (S8) for tile drain 1 (TD1) and storms S5 and S8 for tile drain 2 (TD2). X = to N, for NO<sub>3</sub><sup>-</sup>, NH<sub>4</sub><sup>+</sup> and DON; X = to C, for DOC; X = to P, for TP and SRP.

	$\text{NO}_3^-$	$\text{NH}_4^+$	DON	SRP	TP	DOC
<b>Mean tile flow</b>	0.81*	0.889*	0.399	0.923**	0.919**	0.936**
<b>Bulk Precip</b>	0.857*	0.963**	0.00329	0.848*	0.901*	0.929**

Significance level: \*\* = 0.01, \* = 0.05

**Table 7:** Pearson correlation coefficients between mean tile flow and bulk precipitation and total  $\text{NO}_3^-$ ,  $\text{NH}_4^+$ , dissolved organic nitrogen (DON), soluble reactive phosphorus (SRP), total phosphorus (TP) and dissolved organic carbon (DOC) fluxes for storms 2 (S2), 5 (S5), 6 (S6) and 8 (S8) for tile drain 1 (TD1) and storms S5 and S8 for tile drain 2 (TD2) (n=6).

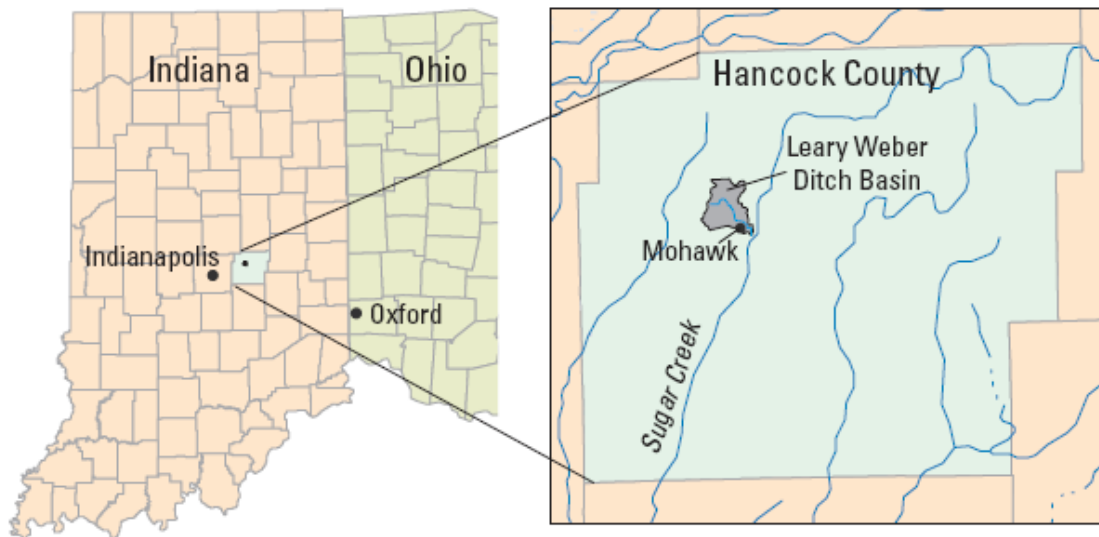


**Figure 1:** Location of Leary Weber Ditch in Indiana. *Modified from Baker et al. (2006).*

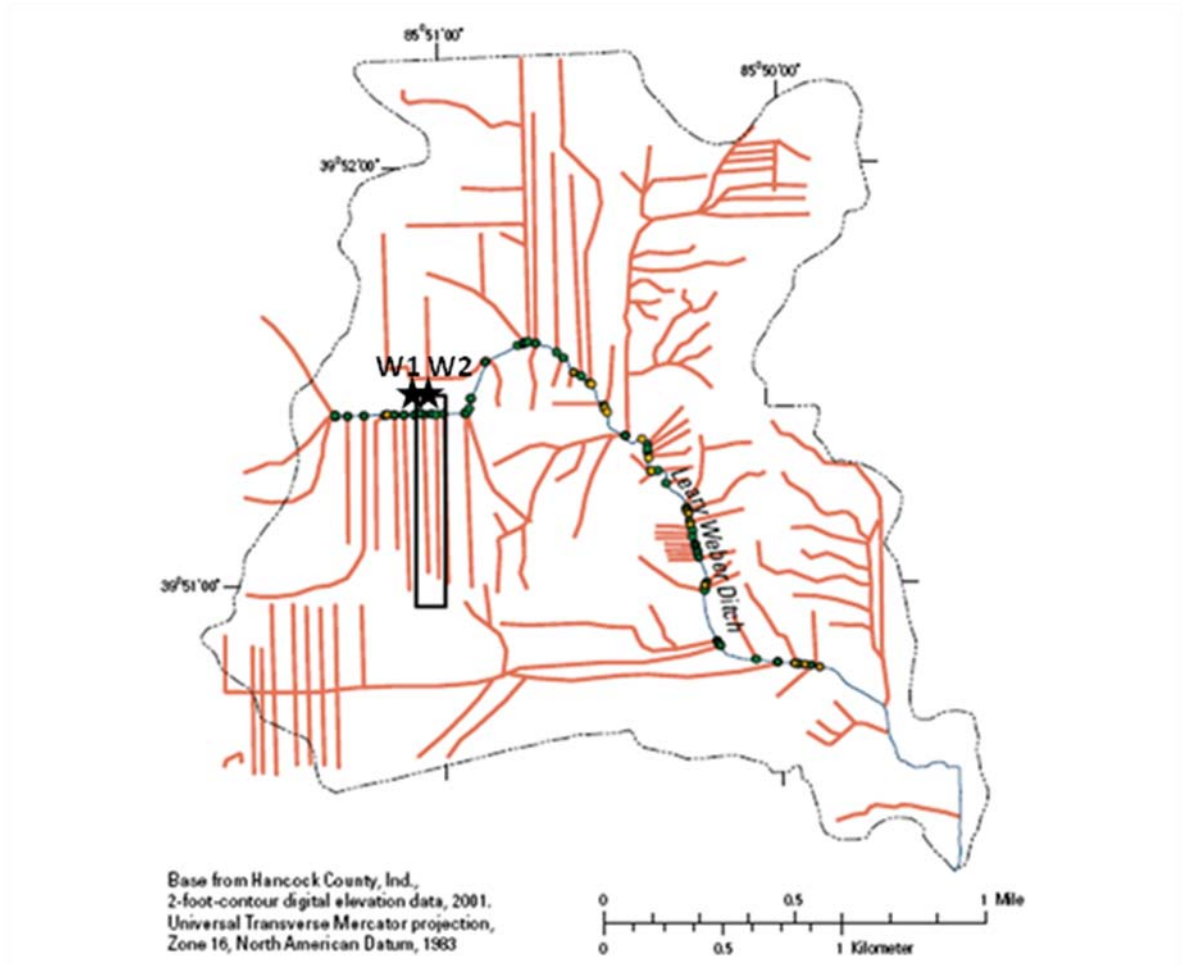


**Figure 2:** Aerial view of the area showing the location and length of the tile drains monitored for this research and the location of groundwater well 1 (W1) and groundwater well 2 (W2). *Modified from Baker et al., (2006).*

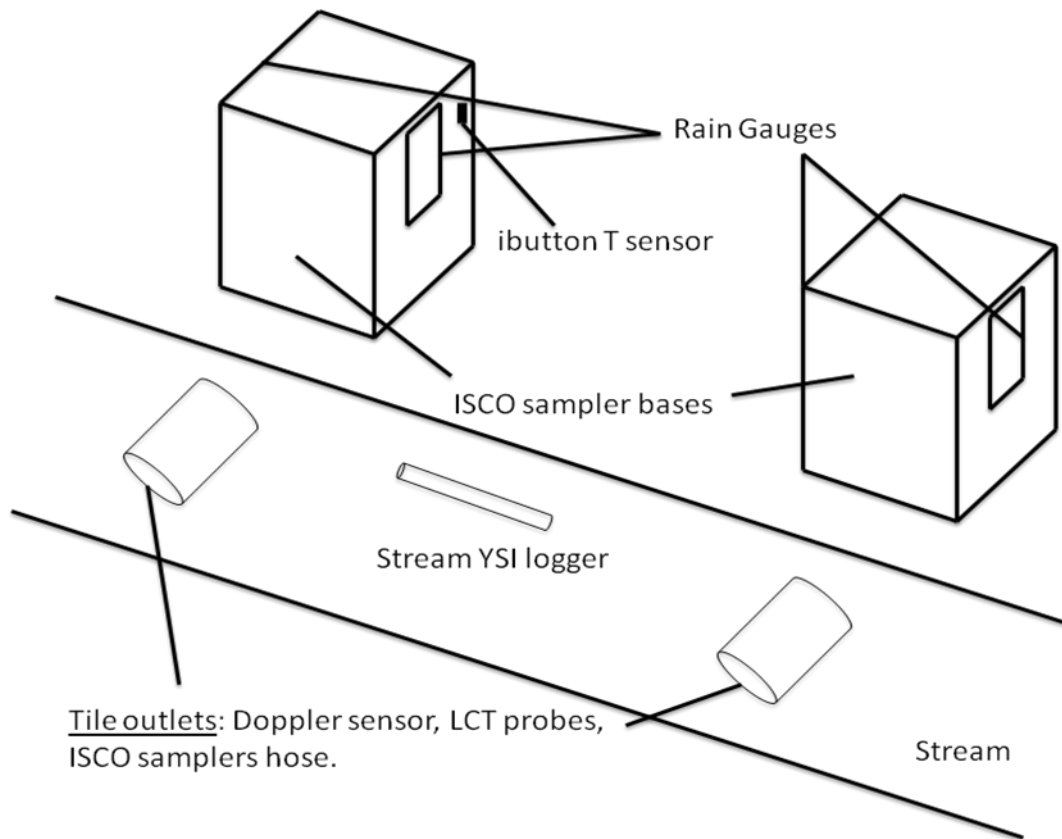
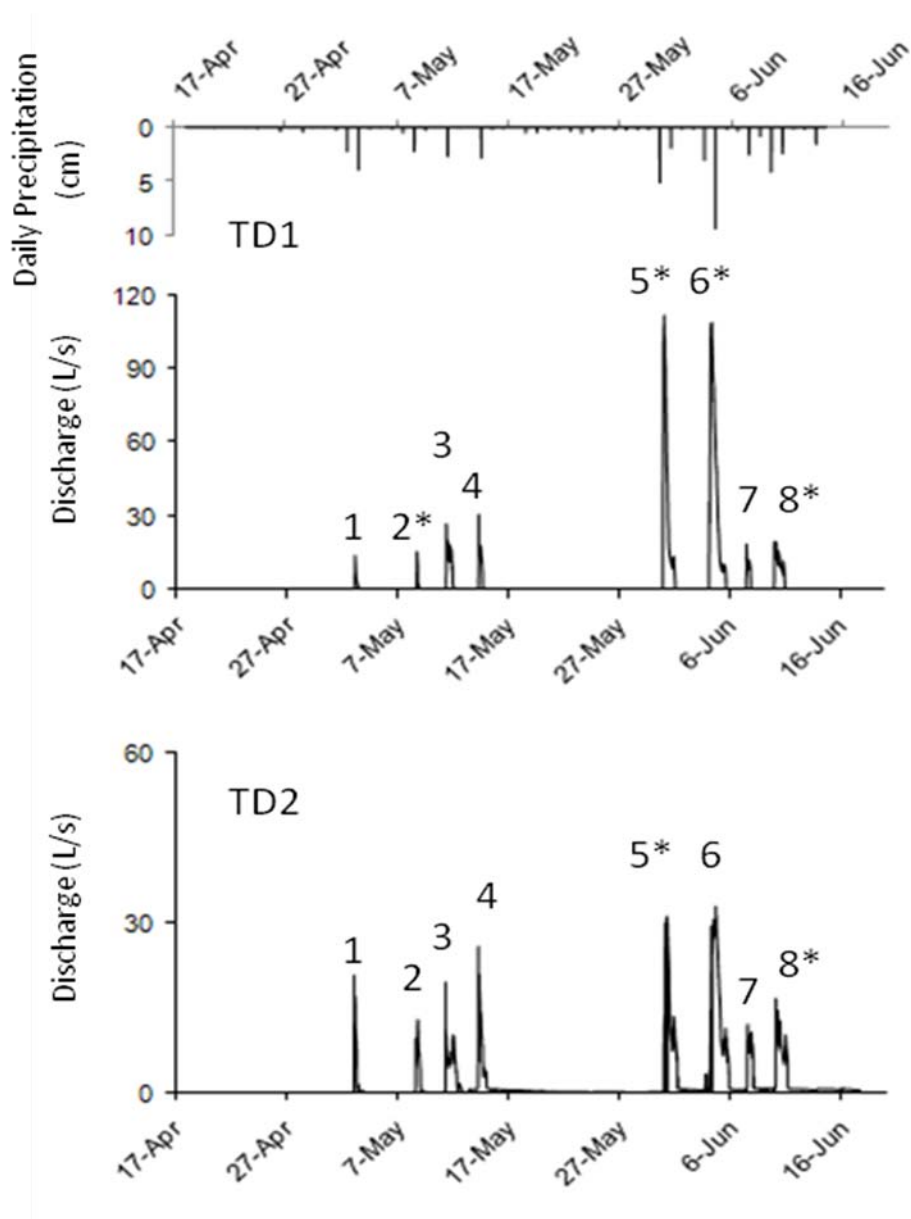


**Figure 3:** Cross section showing the equipment installed in the research site.



\*Water sampling performed for biogeochemical and water quality analysis.

**Figure 4:** Daily precipitation and discharge (20 min interval) in tile drain 1 (TD1) and tile drain 2 (TD2) between April and June 2008. Numbers indicate tile flow events. Tile flow events for which water quality samples were collected are indicated by an asterisk (\*).

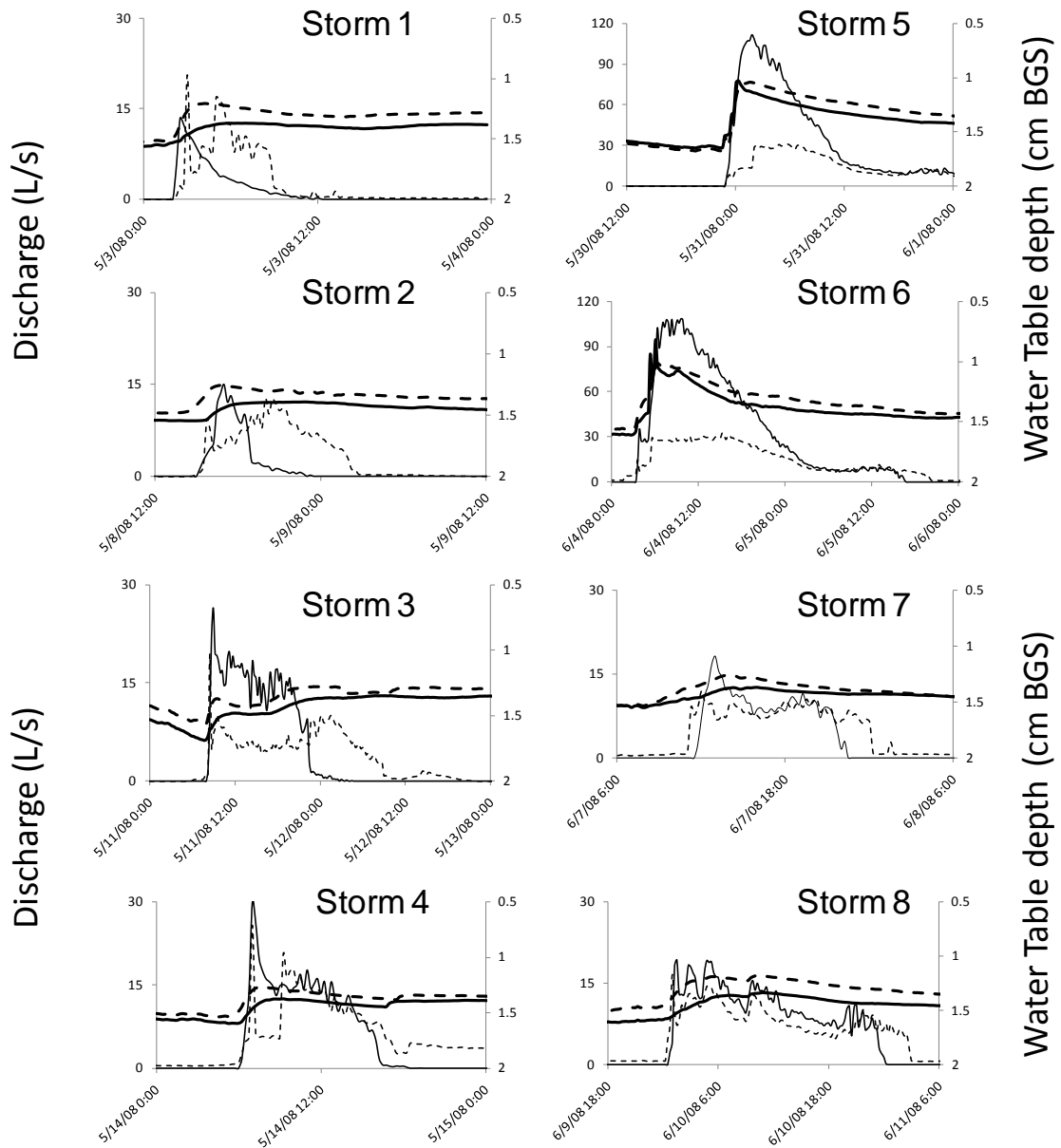


**Figure 5:** Water table depth below ground surface (BGS) in wells 1 and 2 (20 min interval) and discharge in tile drain 1 (TD1) and 2 (TD2) (20 min interval) for storms 1-8 in April-June 2008. Thin solid line indicates discharge in TD1 and thin dashed line indicates discharge on TD2. Thick solid and dashed lines indicate water table level in Well 1 (5 m from TD1) and Well 2 (15 m from TD1), respectively.

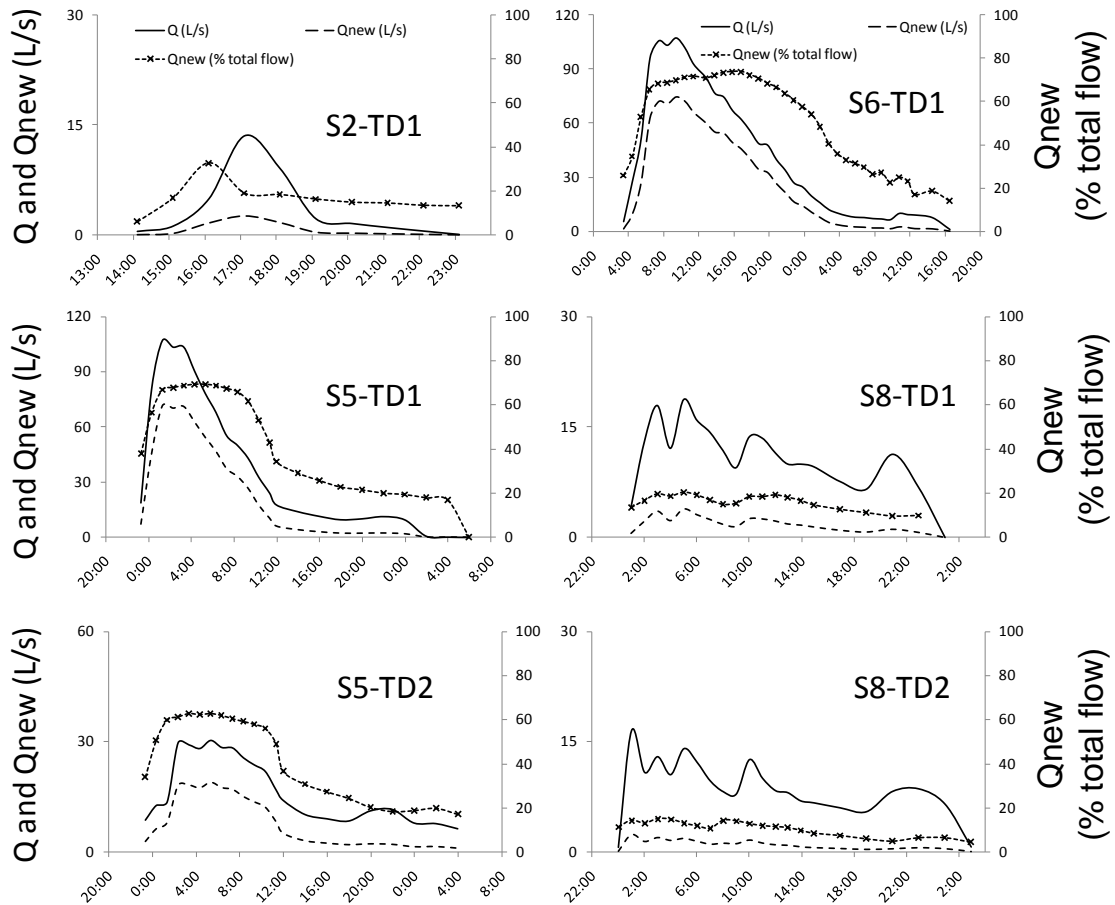


**Figure 6:** Percent of new water contributions with discharge and new water for storms 2 (S2), 5 (S5), 6 (S6) and 8 (S8) for tile drain 1 (TD1) and storm 2 and storm 8 for tile drain 2 (TD2). The solid line represents discharge, the dashed line represents new water and the dashed and dotted line represents the percentage of new water added to tile flow.

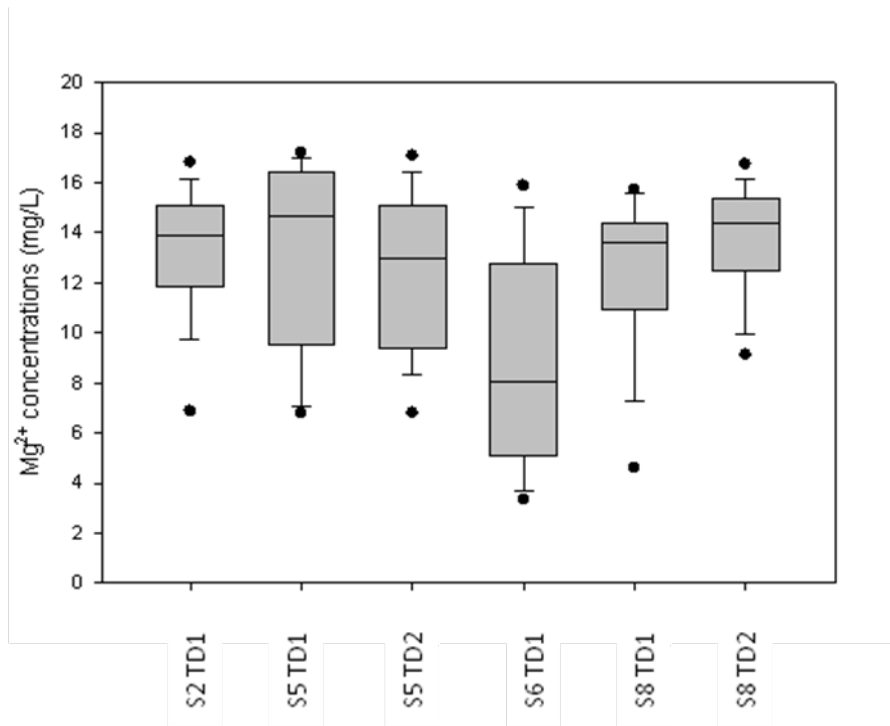


**Figure 7:** Box plots (median, upper (75) and lower (25) quartiles, max, min) showing Mg<sup>2+</sup> concentrations in tile flow during for storms 2 (S2), 5 (S5), 6 (S6) and 8 (S8) for tile drain 1 (TD1) and S2 and S8 for tile drain 2 (TD2).

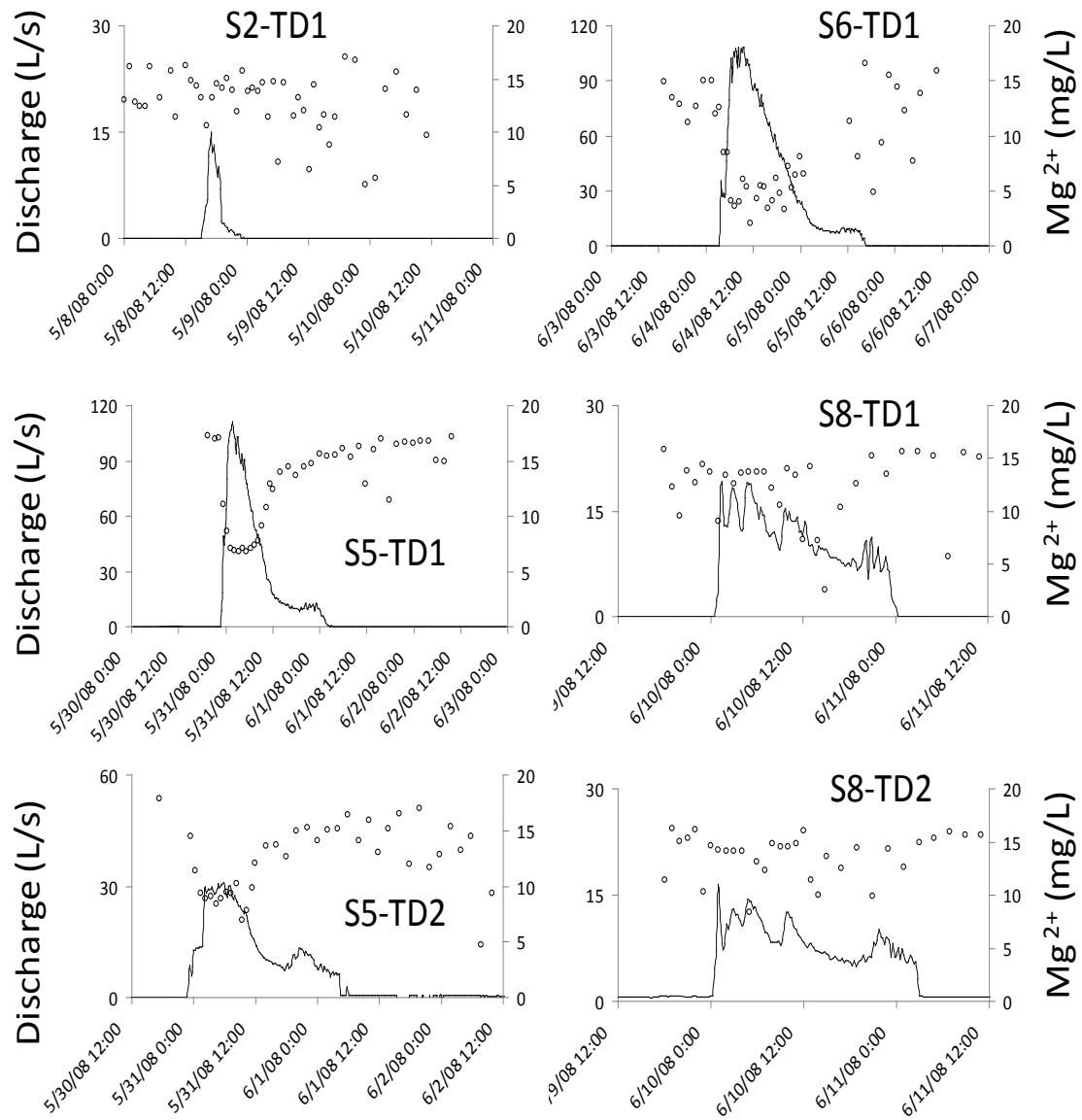


**Figure 8:**  $Mg^{2+}$  and discharge (20 min interval) for storms 2 (S2), 5 (S5), 6 (S6) and 8 (S8) for tile drain 1 (TD1) and for storms S5 and S8 for tile drain 2 (TD2). Solid line indicates discharge. Note the different scales in the Y-axis (discharge).

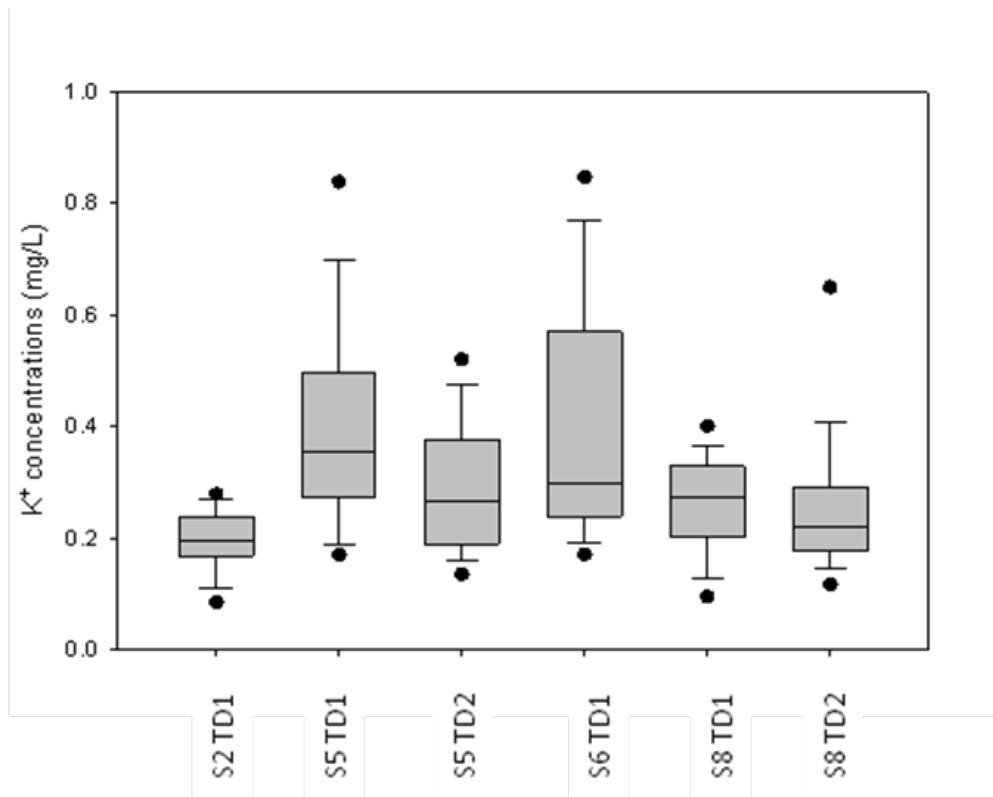


**Figure 9:** Box plots (median, upper (75) and lower (25) quartiles, max, min) showing  $K^+$  concentrations in tile flow during for storms 2, (S2), 5 (S5), 6 (S6) and 8 (S8) for tile drain 1 (TD1) and S2 and S8 for tile drain 2 (TD2).

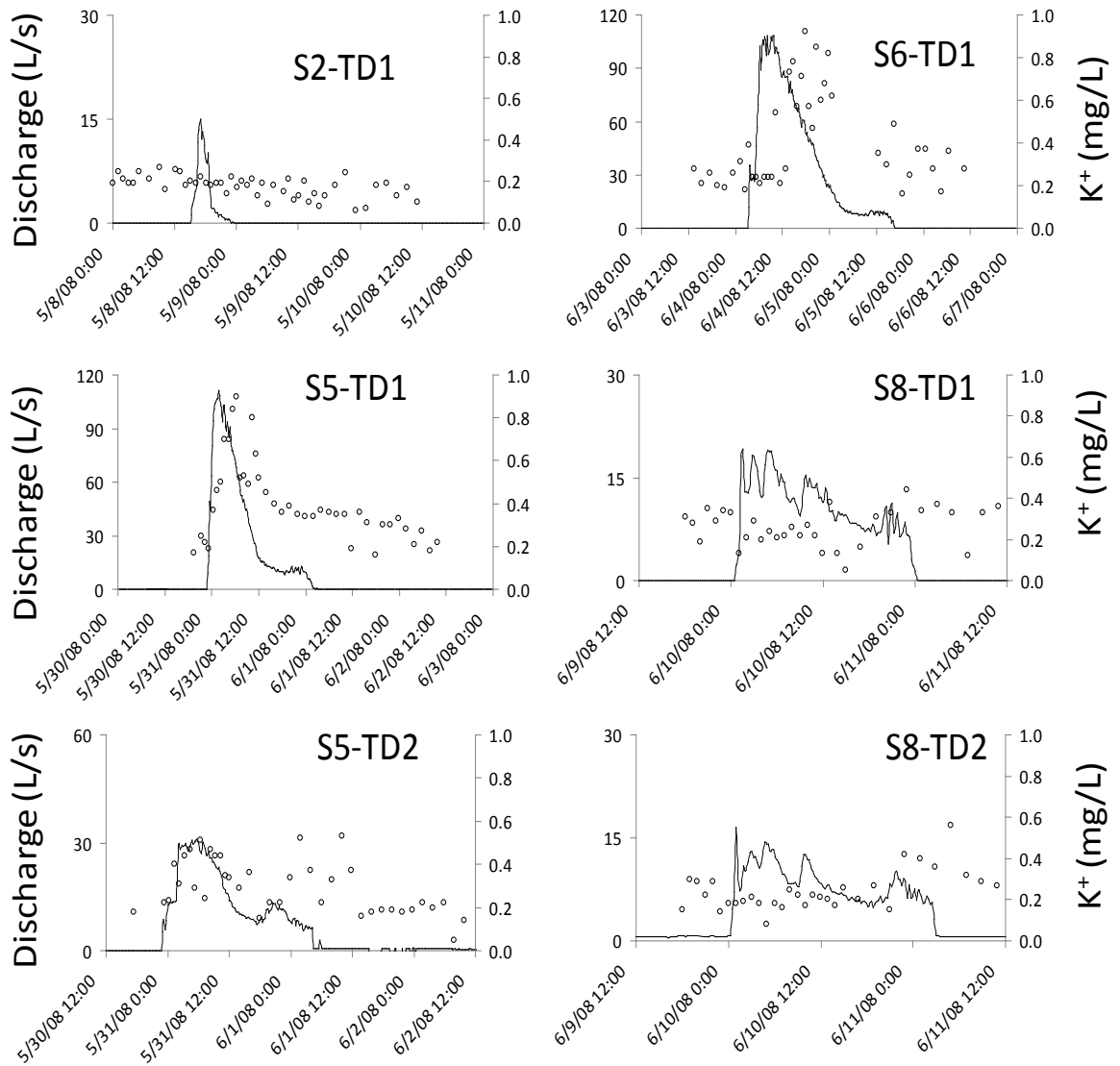


**Figure 10:** K<sup>+</sup> concentrations and discharge (20 min interval) for storms 2 (S2), 5 (S5), 6 (S6) and 8 (S8) for tile drain 1 (TD1) and for storms S5 and S8 for tile drain 2 (TD2). Solid line indicates discharge. Note the different scales in the Y-axis (discharge).

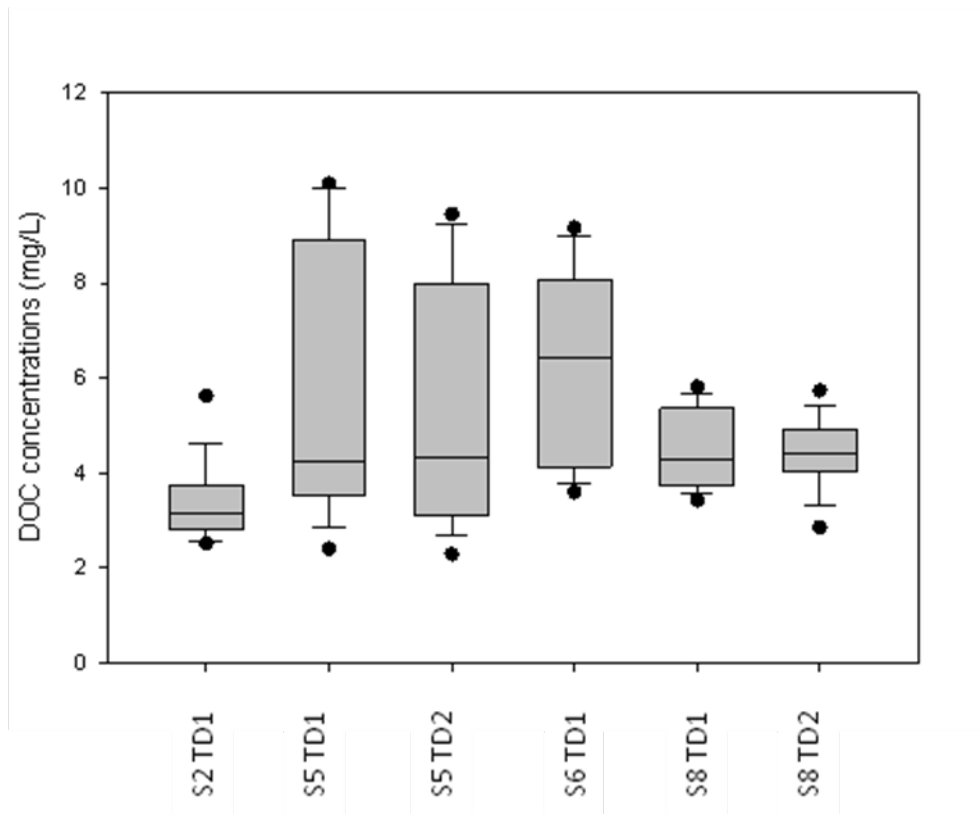


**Figure 11:** Box plots (median, upper (75) and lower (25) quartiles, max, min) showing DOC concentrations in tile flow during for storms 2 (S2), 5 (S5), 6 (S6) and 8 (S8) for tile drain 1 (TD1) and S2 and S8 for tile drain 2 (TD2).

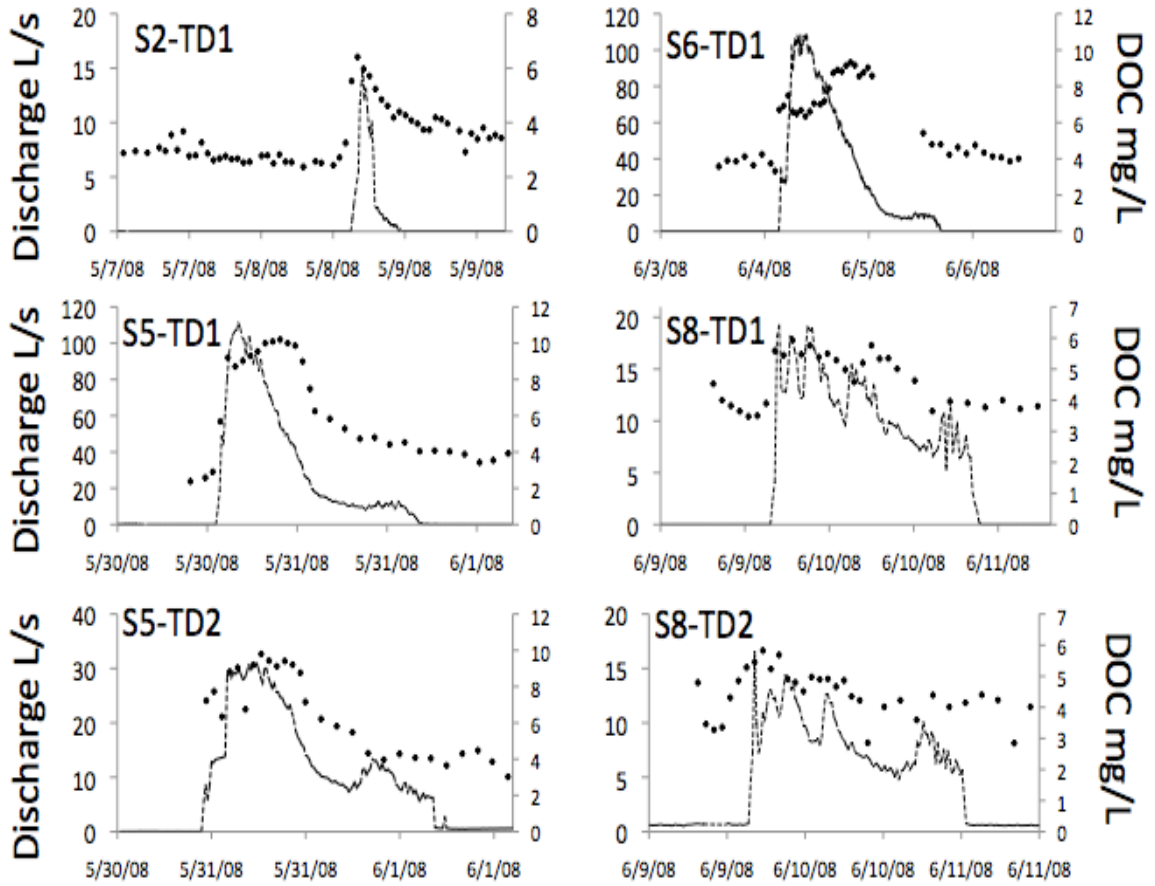


**Figure 12:** DOC concentrations and discharge (20 min interval) for storms 2 (S2), 5 (S5), 6 (S6) and 8 (S8) for tile drain 1 (TD1) and for storms S5 and S8 for tile drain 2 (TD2). Dashed line indicates discharge. Note the different scales in the Y-axis (discharge).

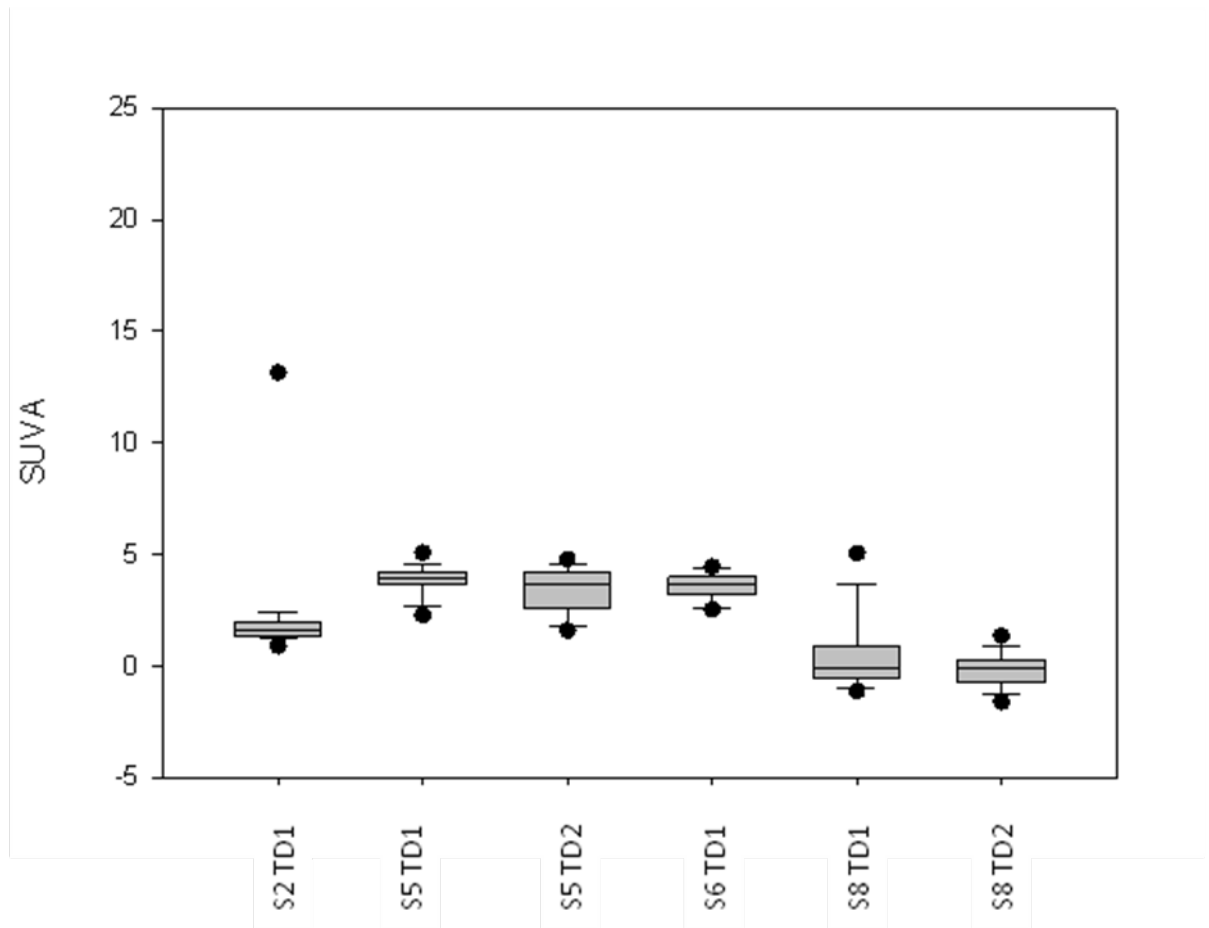


**Figure 13:** Box plots (median, upper (75) and lower (25) quartiles, max, min) showing SUVA values in tile flow during for storms 2 (S2), 5 (S5), 6 (S6) and 8 (S8) for tile drain 1 (TD1) and S2 and S8 for tile drain 2 (TD2).

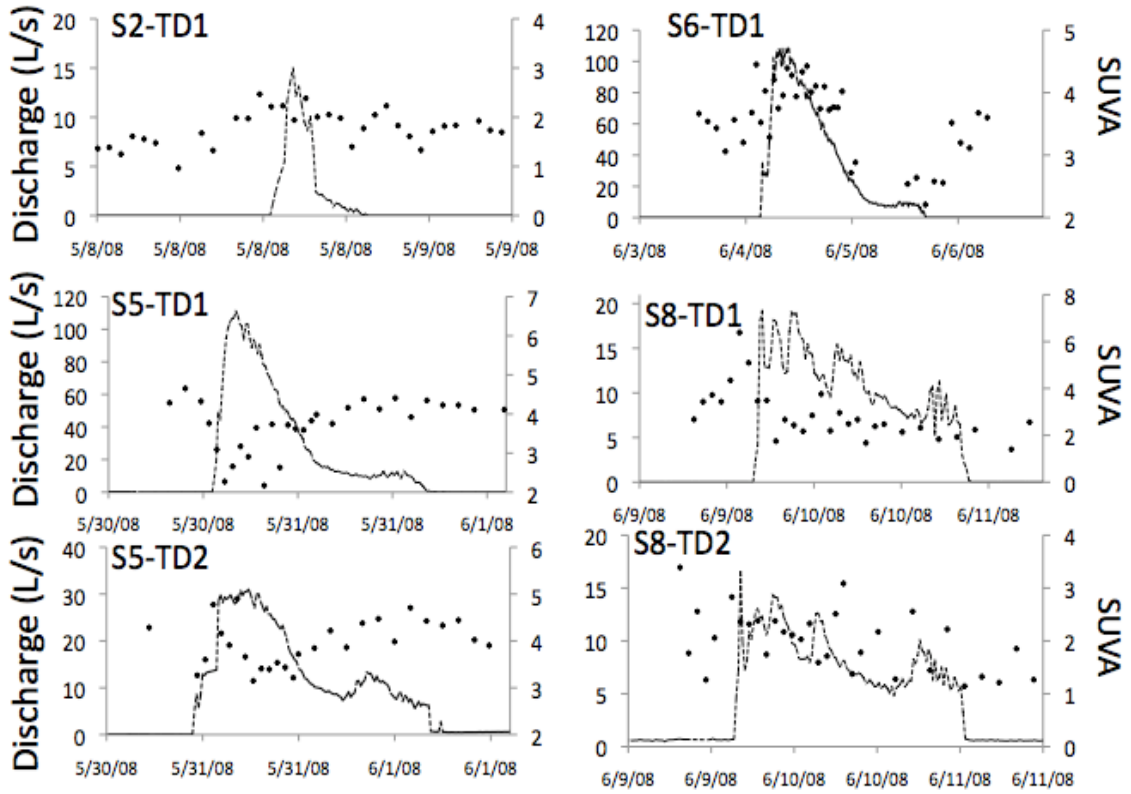


**Figure 14:** SUVA values and discharge (20 min interval) for storms 2 (S2), 5 (S5), 6 (S6) and 8 (S8) for tile drain 1 (TD1) and for storms S5 and S8 for tile drain 2 (TD2). Dashed line indicates discharge. Note the different scales in the Y-axis (discharge).

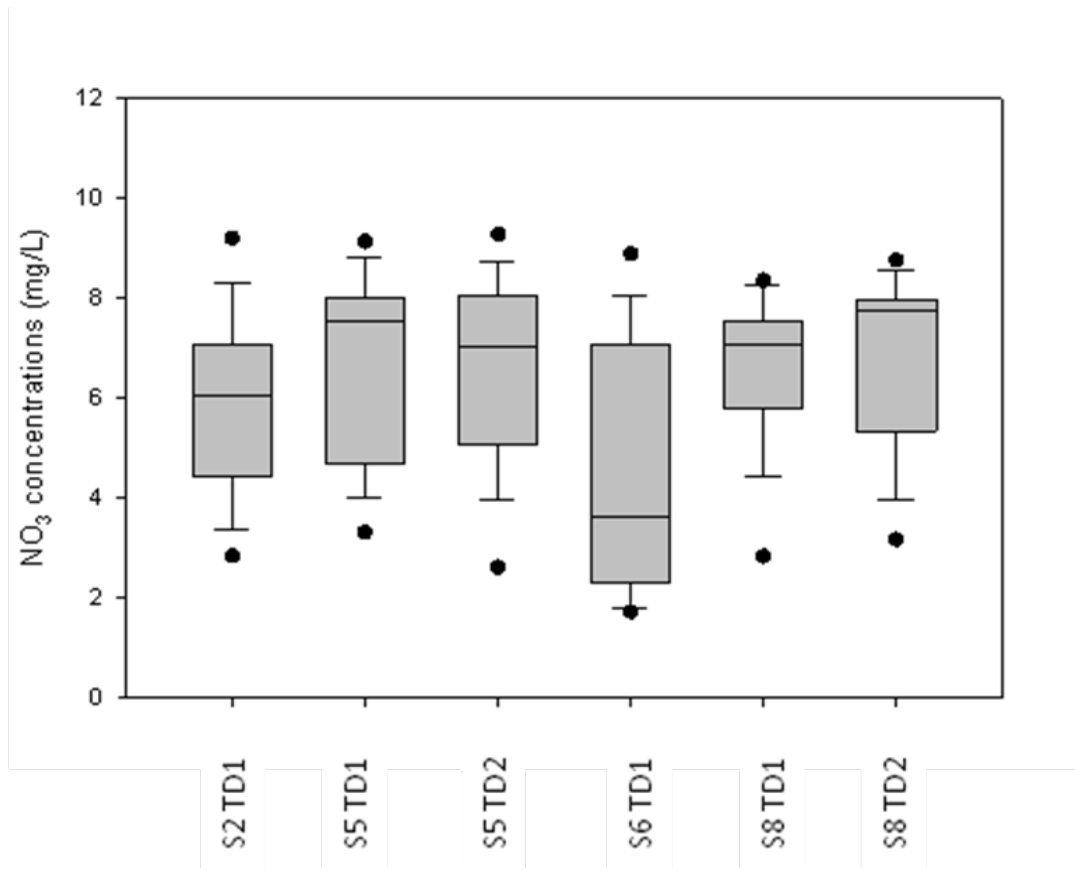


**Figure 15:** Box plots (median, upper (75) and lower (25) quartiles, max, min) showing NO<sub>3</sub><sup>-</sup>-N concentrations in tile flow during for storms 2 (S2), 5 (S5), 6 (S6) and 8 (S8) for tile drain 1 (TD1) and S2 and S8 for tile drain 2 (TD2).

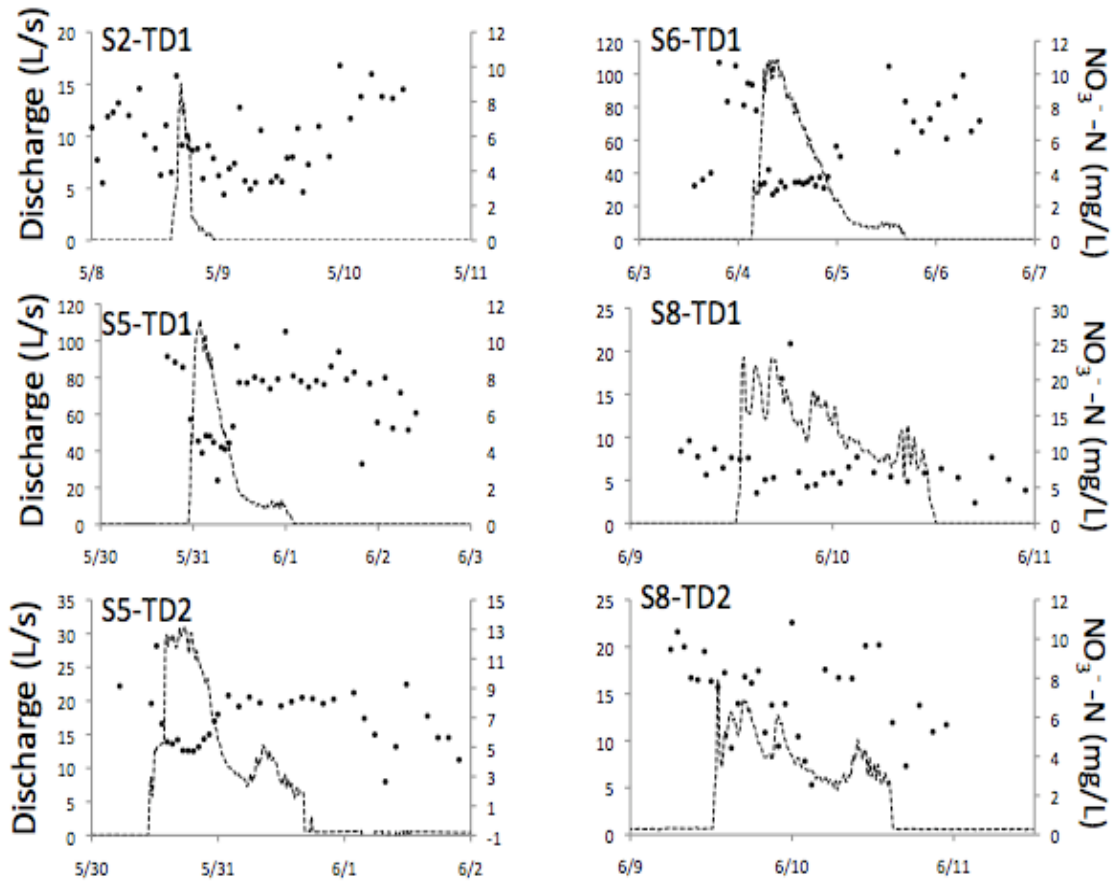


**Figure 16:** NO<sub>3</sub>-N concentrations and discharge (20 min interval) for storms 2 (S2), 5 (S5), 6 (S6) and 8 (S8) for tile drain 1 (TD1) and for storms S5 and S8 for tile drain 2 (TD2). Dashed line indicates discharge. Note the different scales in the Y-axis (discharge).

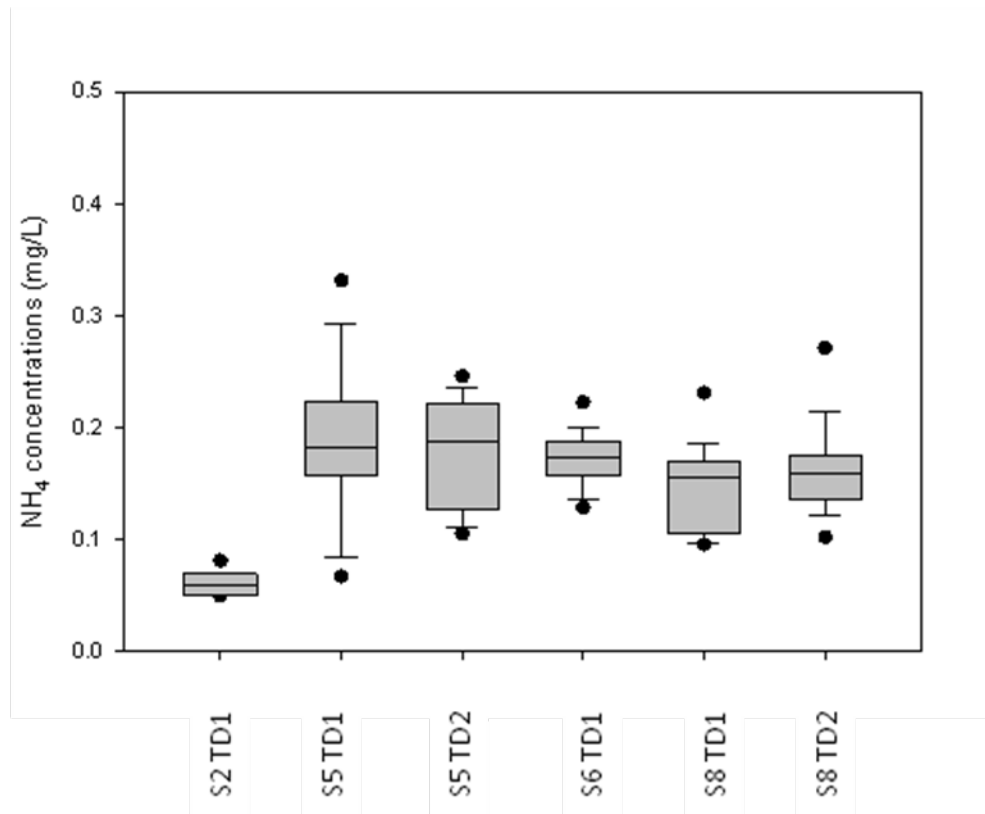


**Figure 17:** Box plots (median, upper (75) and lower (25) quartiles, max, min) showing NH<sub>4</sub><sup>+</sup>-N concentrations in tile flow during for storms 2 (S2), 5 (S5), 6 (S6) and 8 (S8) for tile drain 1 (TD1) and S2 and S8 for tile drain 2 (TD2).

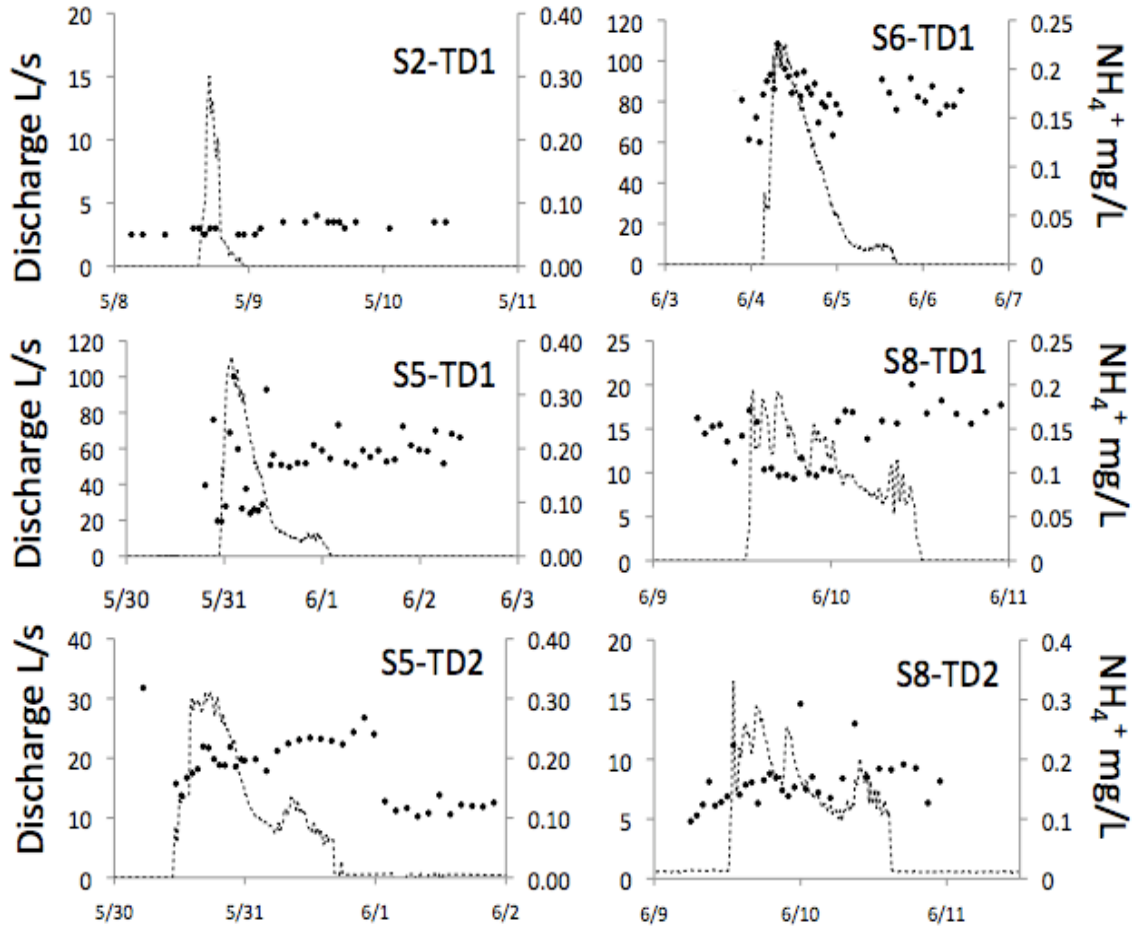


**Figure 18:**  $\text{NH}_4^+\text{-N}$  concentrations and discharge (20 min interval) for storms 2 (S2), 5 (S5), 6 (S6) and 8 (S8) for tile drain 1 (TD1) and for storms S5 and S8 for tile drain 2 (TD2). Dashed line indicates discharge. Note the different scales in the Y-axis (discharge).

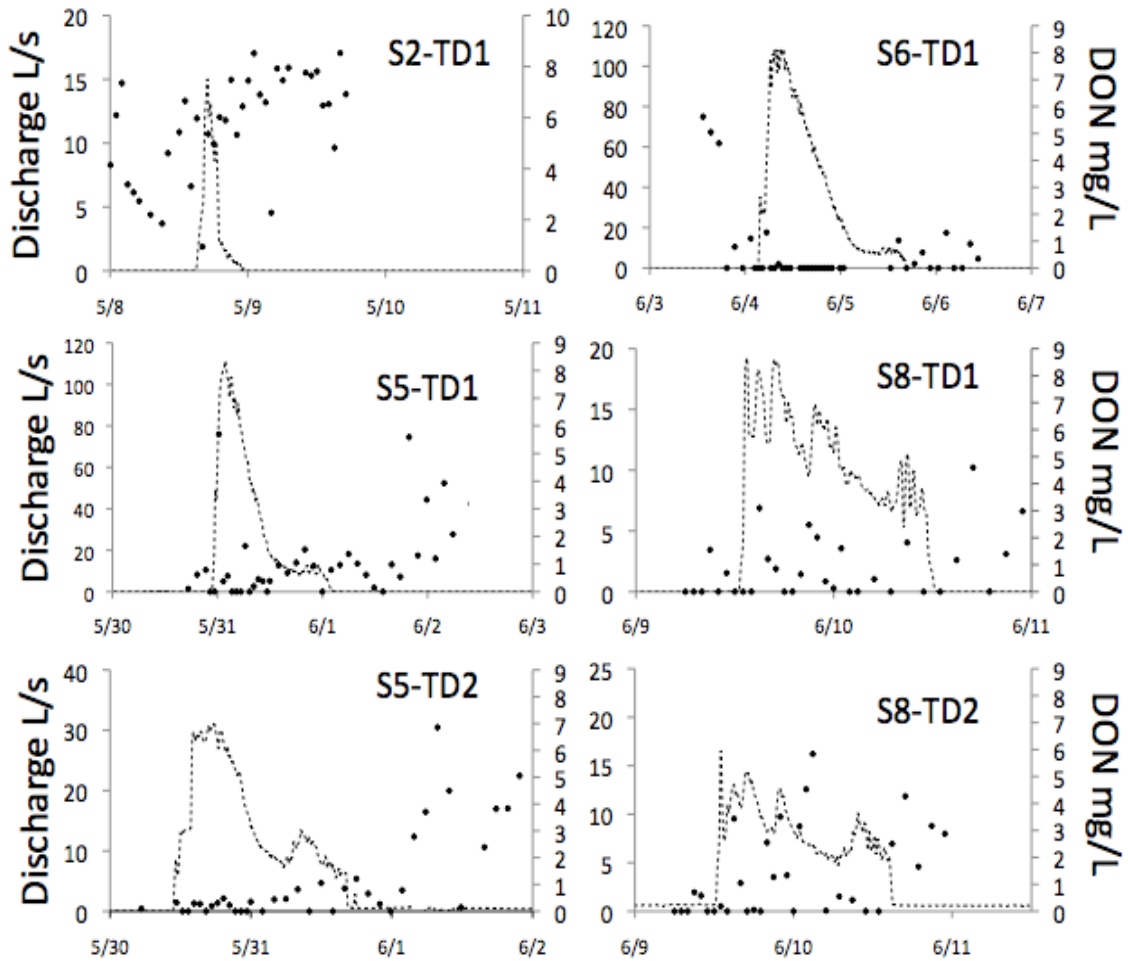


**Figure 19:** DON concentrations and discharge (20 min interval) for storms 2 (S2), 5 (S5), 6 (S6) and 8 (S8) for tile drain 1 (TD1) and for storms S5 and S8 for tile drain 2 (TD2). Dashed line indicates discharge. Note the different scales in the Y-axis (discharge).

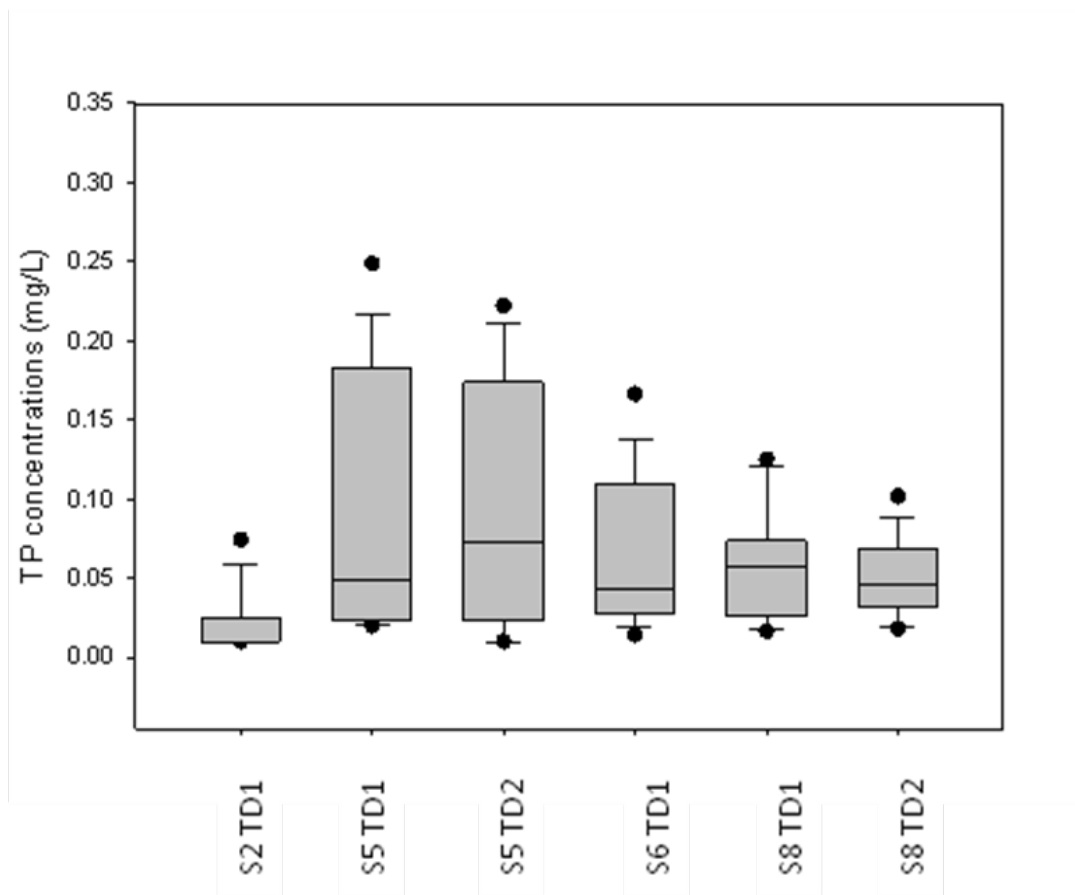


**Figure 20:** Box plots (median, upper (75) and lower (25) quartiles, max, min) showing TP concentrations in tile flow during for storms 2 (S2), 5 (S5), 6 (S6) and 8 (S8) for tile drain 1 (TD1) and S2 and S8 for tile drain 2 (TD2).

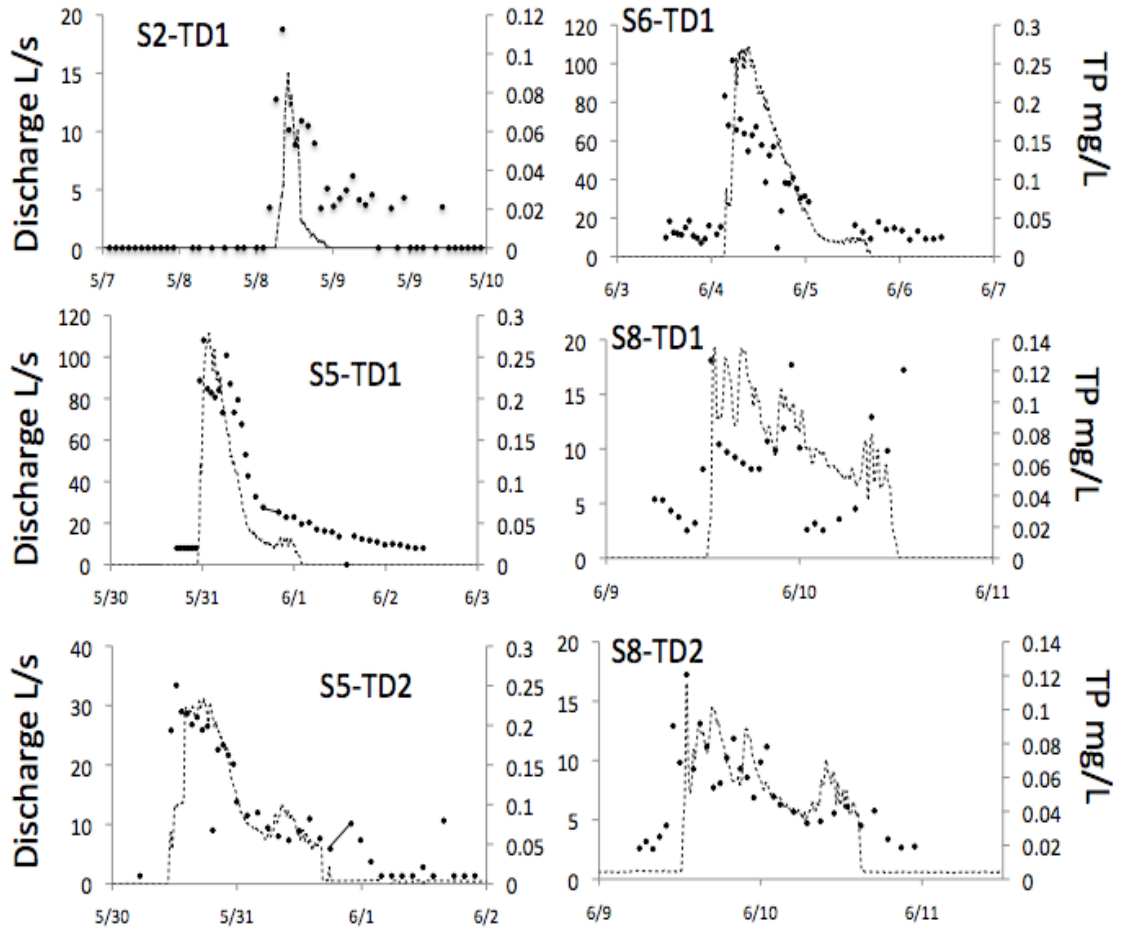


**Figure 21:** TP concentrations and discharge (20 min interval) for storms 2 (S2), 5 (S5), 6 (S6) and 8 (S8) for tile drain 1 (TD1) and for storms S5 and S8 for tile drain 2 (TD2). Dashed line indicates discharge. Note the different scales in the Y-axis (discharge).

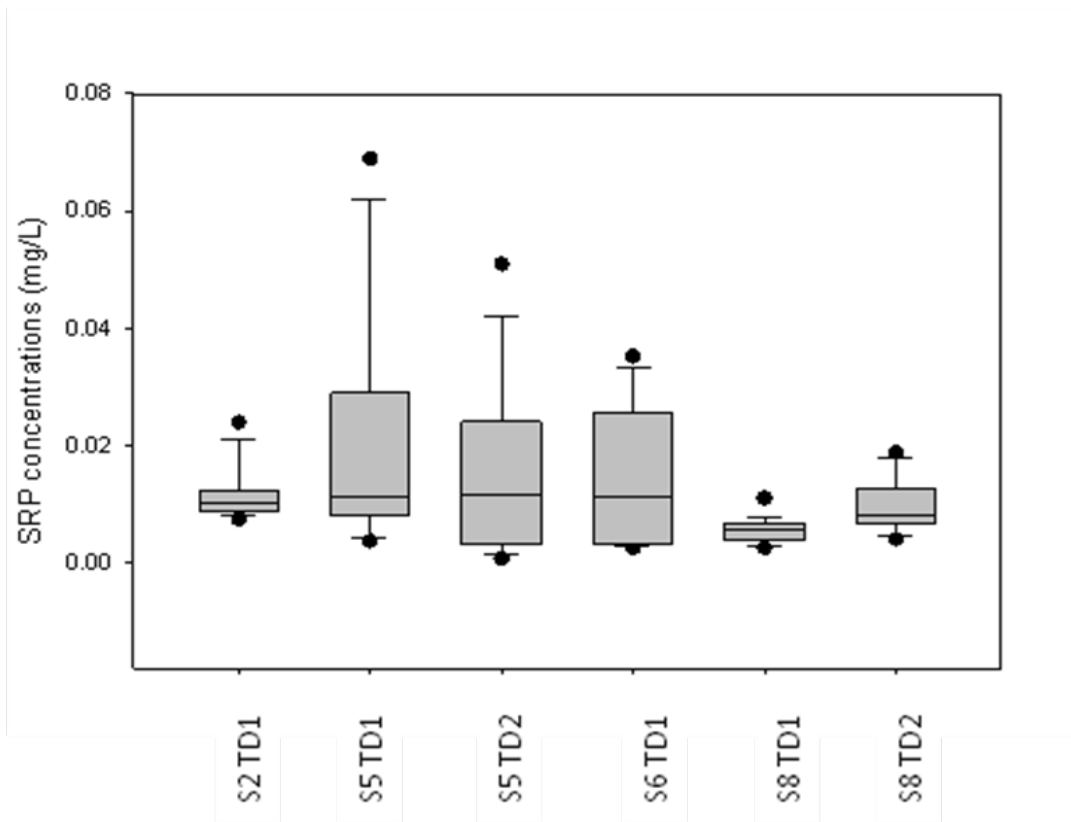


**Figure 22:** Box plots (median, upper (75) and lower (25) quartiles, max, min) showing SRP concentrations in tile flow during for storms 2 (S2), 5 (S5), 6 (S6) and 8 (S8) for tile drain 1 (TD1) and storms S2 and S8 for tile drain 2 (TD2).

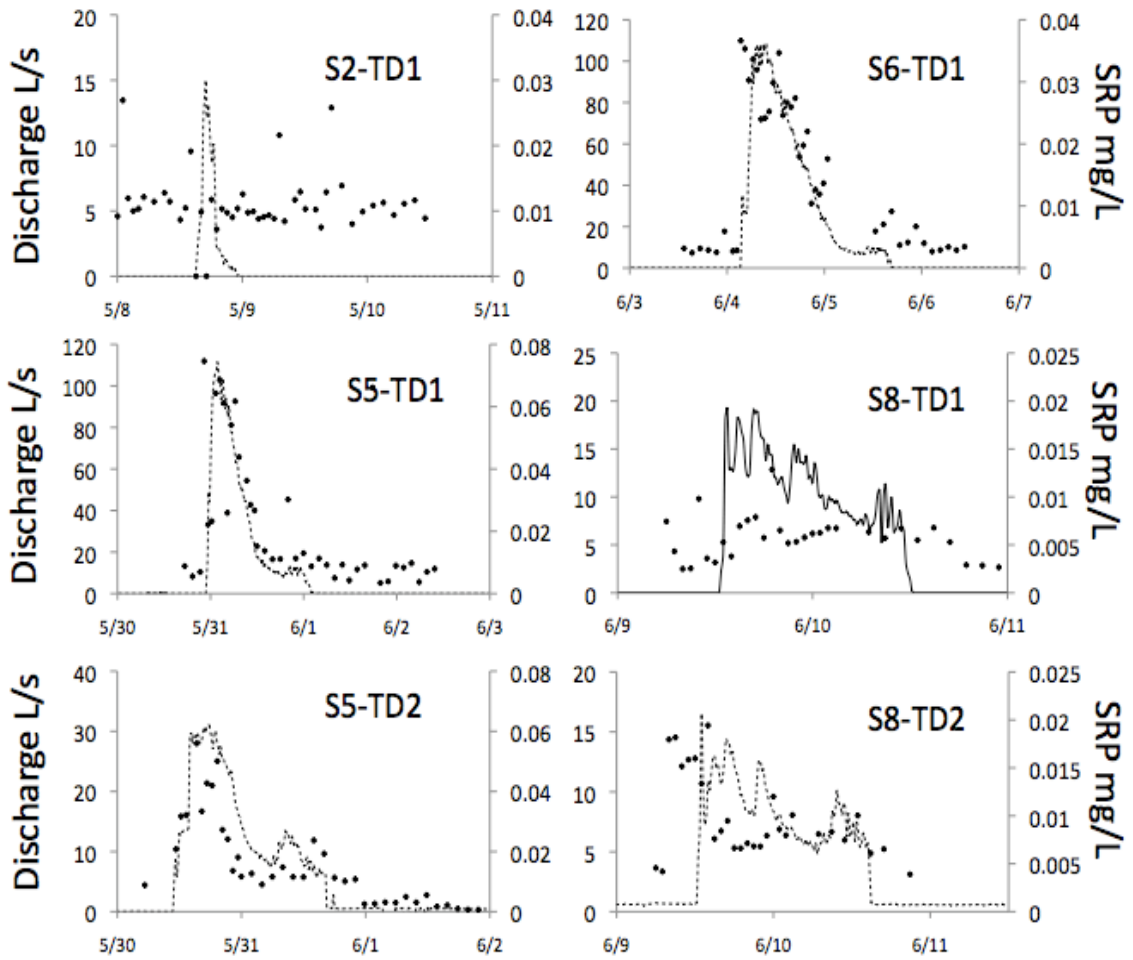


**Figure 23:** SRP concentrations and discharge (20 min interval) for storms 2 (S2), 5 (S5), 6 (S6) and 8 (S8) for tile drain 1 (TD1) and for storms S5 and S8 for tile drain 2 (TD2). Dashed line indicates discharge. Note the different scales in the Y-axis (discharge).

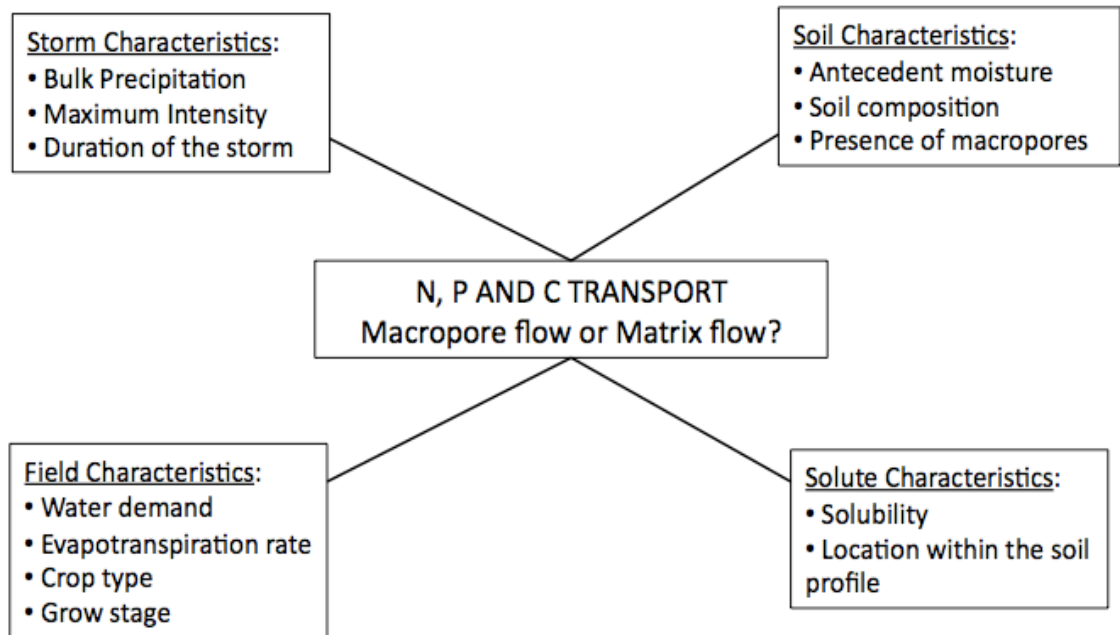


**Figure 24:** Conceptual model for N, P and C transport to tile flow in tile drained fields of central Indiana.

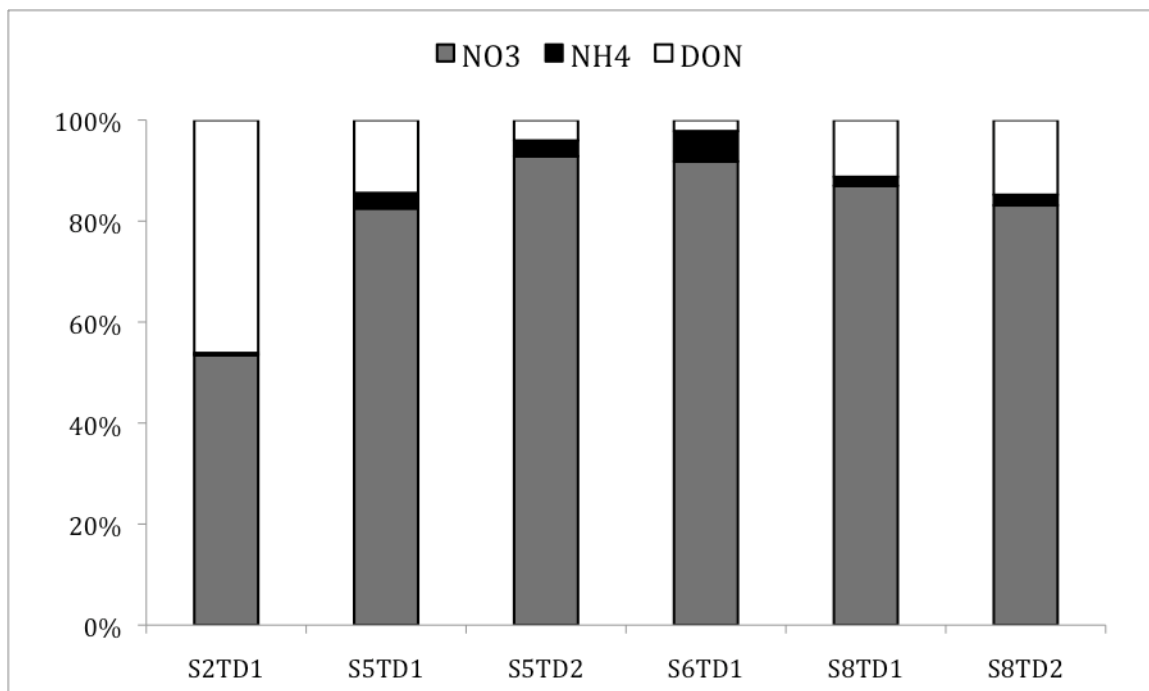


**Figure 25:** Bar graph representing the percentage of  $\text{NO}_3^-$ ,  $\text{NH}_4^+$  and DON in total N fluxes during storms 2 (S2), 5 (S5), 6 (S6) and 8 (S8) for tile drain 1 (TD1) and storms S2 and S8 for tile drain 2 (TD2).

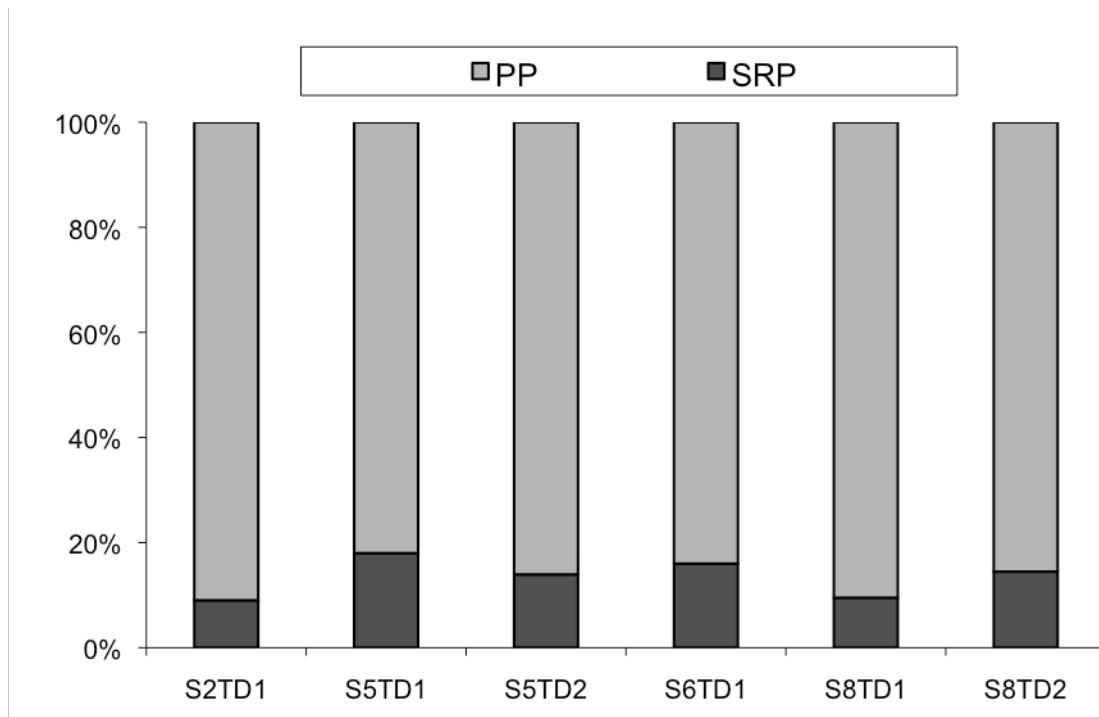


**Figure 26:** Bar graph representing the percentage of soluble reactive phosphorus (SRP) and particulate phosphorus (PP) in total phosphorus (TP) during storms 2 (S2), 5 (S5), 6 (S6) and 8 (S8) for tile drain 1 (TD1) and storms S2 and S8 for tile drain 2 (TD2).

## REFERENCES

- Alexander, R.B., Smith, R.A., Schwarz, G.E., Boyer, E.W., Nolan, J.V. and Brakebill J.W. 2008. Differences in phosphorus and nitrogen delivery to the Gulf of Mexico from the Mississippi River Basin. *Environmental Science Technology* 42, 822-830.
- Baker N.T., W.W., J.T. Wilson and M.T. Meyer. 2006. Occurrence and transport of agricultural chemicals in Leary Weber Ditch Basin, Hancock County Indiana, 2003-04. Geological Survey Scientific Investigation Report 2006-5251, 44 p.
- Baker N.T., W.W. Stone, J.W. Frey and J.T. Wilson, 2007. Water and agricultural-chemical transport in a Midwestern, tile drained watershed: implications for conservation practices. United States Geological Survey, Fact sheet 2007-3084.
- Boyer, E.W., Hornberger, G.M., Bencala, K.E. and McKnight, D.M. 1997. Response characteristics of DOC flushing in an alpine catchment. *Hydrological Processes* 11, 1635-1647.
- Brown, V.A., McDonnell J.J., Burns D.A. and Kendall C. 1999. The role of event water, a rapid shallow flow component, and catchment size in summer stormflow. *Journal of Hydrology* 217, 171-190.
- Creed, I.F. and Band, L.E. 1998. Export of nitrogen from catchments within a temperate forest: evidence for a unifying mechanism regulated by variable source area dynamics. *Water Resources Research* 34.No.11, 3105-3120.
- Dalzell, B.J., T.R. Filley and J.M. Harbor, 2005. Flood pulse influences on terrestrial organic matter export from an agricultural watershed. *Journal of Geophysical Research* 110, G02011, doi: 10.1029/2005JG000043.
- Fox, G.A., Malone, R., Sabbagh, G.J. and Rojas, K. 2004. Interrelationship of macropores and subsurface drainage for conservative tracer and pesticide transport. *Journal of Environmental Quality* 33, 2281-2289.
- Gentry, L.E., David, M.B., Royer, T.V., Mitchell, C.A. and Starks, K.M. 2007. Phosphorus transport pathways to streams in tile-drained agricultural watersheds. *Journal of Environmental Quality* 36, 408-415.
- Goolsby, D.A., Battaglin, W.A., Aulenbach, B.T. and Hooper, R.P. 2002. Nitrogen Input to the Gulf of Mexico. *Journal of Environmental Quality* 30, 329-336.
- Hangen, E., Lindenlaub, M., Leibundgut, C. and Von Wilpert, K. 2001. Investigating mechanisms of stormflow generation by natural tracers and hydrometric data: a small catchment study in the Black Forest, Germany. *Hydrological Processes* 15, 183-199.

- Hart, M.R., Quin, B.F. and Nguyen, M.L. 2004. Phosphorus runoff from agricultural land and direct fertilizer effects: A review. *Journal of Environmental Quality* 33, 1954-1972.
- Hill, A.R and Waddington, J.M. 1993. Analysis of storm run-off sources using oxygen-18 in a headwater swamp. *Hydrological Processes* 7, 305-316.
- Hood, E., Gooseff M.N. and Johnson, S.L. 2006. Changes in the character of stream water dissolved organic carbon during flushing in three small watersheds, Oregon. *Journal of Geophysical Research* 111, G01007, doi:10.1029.
- Inamdar, S.P., Christopher, S.F., and Mitchell M.J. 2004. Export mechanisms for dissolved organic carbon and nitrate during summer storm events in a glaciated forested catchment in New York, USA. *Hydrological Processes* 18:2651-2661.
- Inamdar, S.P. and Mitchell, M.J. 2006. Hydrologic and topographic controls on storm-events exports of dissolved organic carbon (DOC) and nitrate across catchment scales. *Water Resources Research* 42, W03421, doi:10.1029/2005WR004212.
- Indiana State Climate Office. Purdue University, Department of Agronomy. <http://www.agry.purdue.edu/climate/narrative.asp>. Date accessed: April 7<sup>th</sup>, 2009.
- Katsuyama, M. and Ohte, N. 2002. Determining the source of stormflow from the fluorescence properties of dissolved organic carbon in a forested headwater catchment. *Journal of Hydrology* 268, 192-202.
- Katsuyama, M., Ohte, N. and Kobashi, S. 2001. A three-component end-member analysis of streamwater hydrochemistry in a small Japanese forested headwater catchment. *Hydrological Processes* 15, 249-260.
- Kladivko, E.J., Van Scoyoc, G.E., Monke, E.J., Oates, K.M. and Pask, W. 1991. Pesticide and nutrient movement into subsurface tile drains on a silt loam soil in Indiana. *Journal of Environmental Quality* 20, 264-270.
- Kladivko E.J., Grochulska, J., Turco, R.F., Van Scoyoc, G.E. and Eigel, J.D. 1999. Pesticide and nitrate transport into subsurface tile drains of different spacing. *Journal of Environmental Quality* 28, 997-1004.
- Kladivko, E.J., Brown, L.C and Baker, J.L. 2001. Pesticide transport to subsurface tile drains in humid regions of North America. *Critical Reviews in Environmental Science and Technology* 31(1), 1-62.
- Krug, E. C. 2007. Coastal change and hypoxia in the northern Gulf of Mexico: Part I. *Hydrology and Earth Systems Sciences* 11, 180-190.

- Kung, K.J.S., Steenhuis, T.S., Kladivko, E.J., Gish, T.J., Bubenzer, G. and Helling, C.S. 2000. Impact of preferential flow on the transport of adsorbing and non-adsorbing tracers. *Soil Science Society of American Journal* 64, 1290-1296.
- Liu, F., Williams M.W. and Caine N. 2004. Source waters and flow paths in an alpine catchment, Colorado Front Range, United States. *Water Resources Research* 40, W09401, doi:10.1029/2004WR003076.
- McHale, M.R., McDonnell, J.J., Mitchell, M.J. and Cirimo, C.P. 2002. A field-based study of soil water and groundwater nitrate release in an Adirondack forested watershed. *Water Resources Research* 38, No.4, doi:10.1029/2000WR000102.
- McDowell, R.W. and Wilcock, R.J. 2004. Particulate phosphorus transport within stream flow of an agricultural catchment. *Journal of Environmental Quality* 33, 2111-2121.
- McIsaac, G.F., David, M.B., Gertner, G.Z., and Goolsby, D.A. 2002. Relating net nitrogen input in the Mississippi River Basin to nitrate flux in lower Mississippi River: A comparison of approaches. *Journal of Environmental Quality* 31, 1610-1622.
- NOAA, climatological data, Indianapolis. National Oceanic and Atmospheric Administration, National Climatic Data Center:  
<http://www.crh.noaa.gov/ind/climatenormals.txt>. Date accessed: Jan 16, 2005.
- Poor, C.J. and McDonnell, J.J. 2007. The effects of land use on stream nitrate dynamics. *Journal of Hydrology* 332, 54-68.
- Randall, G.W. and Mulla, D.J. 2001. Nitrate nitrogen in surface waters as influenced by climatic conditions and agricultural practices. *Journal of Environmental Quality* 30, 337-344.
- Royer, T.V. and David, M.B. 2005. Export of dissolved organic carbon from agricultural streams in Illinois, USA. *Aquatic Sciences* 67, 465-471.
- Royer, T.V., David, M.B. and Gentry, L.E. 2006. Timing of riverine export of nitrate and phosphorus from agricultural watersheds in Illinois: Implications for reducing nutrient loading to the Mississippi River. *Environmental Science and Technology* 40, 4126-4131.
- Scott, D., Harvey, J., Alexander, R. and Schwarz, G. 2007. Dominance of organic nitrogen from headwater streams to large rivers across the conterminous United States, *Global Biogeochemistry Cycles* 21, GB1003, doi:10.1029/2006GB002730.
- Sidle, R.C., Tsuboyama Y., Noguchi, S., Hosoda, I., Fujieda, M. and Shimizu, T. 2000. Stormflow generation in steep forested headwaters: a linked hydrogeomorphic paradigm. *Hydrological Processes* 14, 369-385.

Stone, W.W. and Wilson, J.T. 2006. Preferential flow estimates to an agricultural tile drain with implications for Glyphosate Transport. *Journal of Environmental Quality* 35, 1825-1835.

Turgeon, J. M. L. and Courchesne F. 2008. Hydrochemical behavior of dissolved nitrogen and carbon in headwater stream of the Canadian Shield: relevance of antecedent soil moisture. *Hydrological Processes* 22, 327 -339.

Vidon, P., Wagner, L.E. and Soyeux, E. 2008a. Changes in the character of DOC in streams during storms in two Midwestern watershed with contrasting land uses. *Biogeochemistry*, doi:10.1007/s10533-008-9207-6.

Vidon, P., Hubbard, L.E. and Soyeux, E. 2008b. Impact of sampling strategy on stream load estimates in till landscape of the Midwest. *Environmental Monitoring Assess* DOI 10.1007/s10661-008-0635-5.

Vidon, P, Hubbard L.E and Soyeux E. 2009. Seasonal solute dynamics across land uses during storms in glaciated landscape of the U.S. Midwest. *Journal of Hydrology* 376, 34-47.

Ward, A.D. and Trimble, S.W. 2004. *Environmental Hydrology Second Edition*. Lewis Publishers. USA.

Weishaar, J.L., Aiken, G.R., Depaz, E., Bergamaschi, B., Fram, M. and Fujii, R. 2003. Evaluation of specific ultra-violet absorbance as an indicator of the chemical composition and reactivity of dissolved organic carbon. *Environmental Science and Technology* 37, 4702-4708.

## CURRICULUM VITAE

Pilar E. Cuadra

### **Education**

- 1/08-12/09 M.S., Earth Sciences, concentration in Hydrology  
Indiana University, Indianapolis, Indiana.  
*Thesis:* IMPACT OF PRECIPITATION CHARACTERISTICS IN  
NUTRIENT AND CARBON DELIVERY TO STREAMS IN  
ARTIFICIALLY DRAINED LANDSCAPES OF THE MIDWEST
- 9/02-5/07 B.S., Geophysical Engineering.  
Universidad Simon Bolivar, Caracas, Venezuela.

### **Professional Experience**

- 1/08-12/09 Research Assistant/Graduate Student, Indiana University.  
Indianapolis, Indiana.
- 5/07-9/07 Geophysics Department Summer Intern, Mundell and Associates.  
Indianapolis, Indiana.
- 9/06-4/07 Geophysical Assistant, TRX Consulting.  
Caracas, Venezuela.

### **Publications and Presentations**

- P. Vidon and Cuadra P. E. (2009). Impact of precipitation characteristics on soil hydrology in tile-drained landscapes. Submitted.

Cuadra P. E. and P. Vidon (2009). Natural Variability in Dissolved Organic Carbon and Dissolved Organic Nitrogen Transport in Artificially Drained Landscapes of the U.S. Midwest. American Geophysical Union Joint Assembly, Toronto, Ontario, Canada, May 2009.

### **Awards and Honors**

2009            IUPUI Graduate Student Organization Travel Grant Award.  
2008/2009     Mirsky Fellowship Recipient.